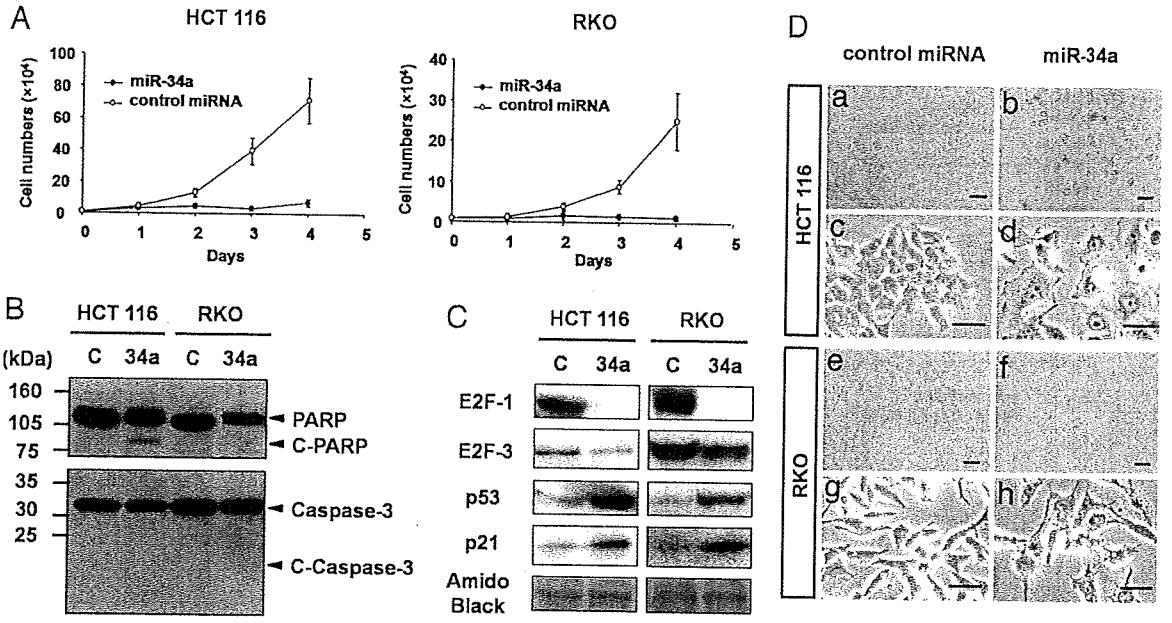

Fig. 2. *miR-34a* inhibits cell proliferation and induces senescence-like phenotypes through down-regulation of E2F and up-regulation of p53/p21 in HCT 116 and RKO cells. (*A*) HCT 116 and RKO cells, seeded at 1.0×10^4 cells in 24-well plates, were transfected with control miRNA (open circles) or *miR-34a* (filled circles) on day 0, and cells were counted on the days indicated. The data are expressed as mean values with standard deviations. Cultures were performed in triplicate. (*B*) Immunoblot analysis of apoptotic cell markers. Cell extracts from HCT 116 and RKO cells were subjected to immunoblot analysis by using anti-PARP and anti-caspase-3 antibodies. Lanes C and 34a indicate the lysates of cells transfected with control miRNA and *miR-34a*, respectively. The molecular sizes of the intact and cleaved forms of PARP (*Upper*) and those of caspase-3 (*Lower*) are indicated on the right. (*C*) Cells transfected with control miRNA (C) and *miR-34a* (34a) were incubated for 3 days, and cell lysates were then subjected to immunoblot analysis. Amido black staining for an 80-kDa protein in the immunoblot is shown as a protein loading control. Marked down-regulation of E2F-1 and -3, and up-regulation of p53 and p21 were observed after *miR34a* transfection in both HCT 116 and RKO cells. (*D*) Induction of senescence-like appearance in cells by *miR-34a*. Cells transfected with control miRNA (*a*, *c*, *e*, and *g*) or *miR-34a* (*b*, *d*, *f*, and *h*) were subjected to SA-β-gal staining. *a*, *b*, *e*, and *f* are low-magnification images for visualizing SA-β-gal-positive cells, and *c*, *d*, *g*, and *h* are high-magnification images for morphological observation. (Scale bars, 10 μm.)

served that p53-mutated human colon cancer cells exhibited morphological changes and SA-β-gal positive staining characteristic of cellular senescence (SI Fig. 5). These results suggest that suppression of cell proliferation by *miR-34a* is mainly associated with the induction of senescence-like phenotypes.

Administration of *miR-34a* with Atelocollagen Suppresses Tumor Growth *in Vivo*. Atelocollagen has been recently shown to be a very useful system to efficiently deliver small interfering RNA molecules into tumors *in vivo* (15–17). Subcutaneous administration of *miR-34a*/atelocollagen complexes caused significant suppression of growth of both HCT 116 and RKO cells by day 4 compared with the administration of the control miRNA/atelocollagen complex (Fig. 3). Significant reduction of tumor volume was also observed for HCT 116 cells until day 6 after the *miR-34a* administration. The averaged tumor volumes were decreased significantly with administration of *miR-34a* compared with those that were administered control miRNA throughout the entire experimental period of 14 days. Tumor tissues treated with *miR-34a* showed a considerable amount of necrotic tissue but showed no significant differences in Ki67 and p21 immunostaining compared with those treated with control miRNA (SI Fig. 6). These results indicate that introduction of *miR-34a* suppresses the growth of human colon cancer cells to tumors in an *in vivo* setting as well.

A Subset of Human Colon Cancers Shows Decreased *miR-34a* Expression. To gain insight into the biological role of *miR-34a* in human colon carcinogenesis, we analyzed the expression of *miR-34a* in human colon cancer and paired counterpart normal tissue (Fig. 4). Nine of 25 colon cancer tissues (36%) (patient IDs 2, 5, 9, 10, 12, 16, 18, 20, and 22) showed decreased expression of *miR-34a*, suggesting that down-regulation of *miR-34a* may be, at least in part, involved in human colon cancer development.

Discussion

Altered expression of *microRNA* genes has recently been reported to impact human carcinogenesis (7–9). In the present study, *miR-34a* was identified as a DNA damage-responsive gene in the HCT 116 colon cancer cell line after treatment with a low concentration of ADR, at which cell proliferation is completely arrested without substantial induction of apoptosis (18). The induction of *miR-34a* by ADR treatment led us to hypothesize that *miR-34a* is a responsive gene for chemically induced cellular stress. This hypothesis is supported by recent reports that *miR-34a* is up-regulated by treatment with sodium arsenite in human immortalized lymphoblasts (19) and with tamoxifen in rat hepatocytes (20).

The introduction of *miR-34a* into two colon cancer cell lines, HCT 116 and RKO, showed a profound inhibition of cell proliferation accompanying the down-regulation of the E2F family. The E2F family is a well characterized group of transcription factors comprising eight subclasses, E2F1–E2F8 (21). E2F1–E2F3 are positive regulators for the cell cycle, whereas E2F4 and -5 negatively regulate, and the functions of E2F6–8 are unknown. Embryonic fibroblasts derived from knockout mice lacking *E2f1*, *-2*, or *-3* demonstrate slow cell-cycle progression, especially at entry to the S phase (22, 23), but there is not a complete block of the cell cycle and of proliferation. In contrast, fibroblasts with triple knockout of *E2f1–E2f3* demonstrate strong inhibition of cell proliferation throughout the cell cycle. Interestingly, induction of p53 and its downstream target p21 was

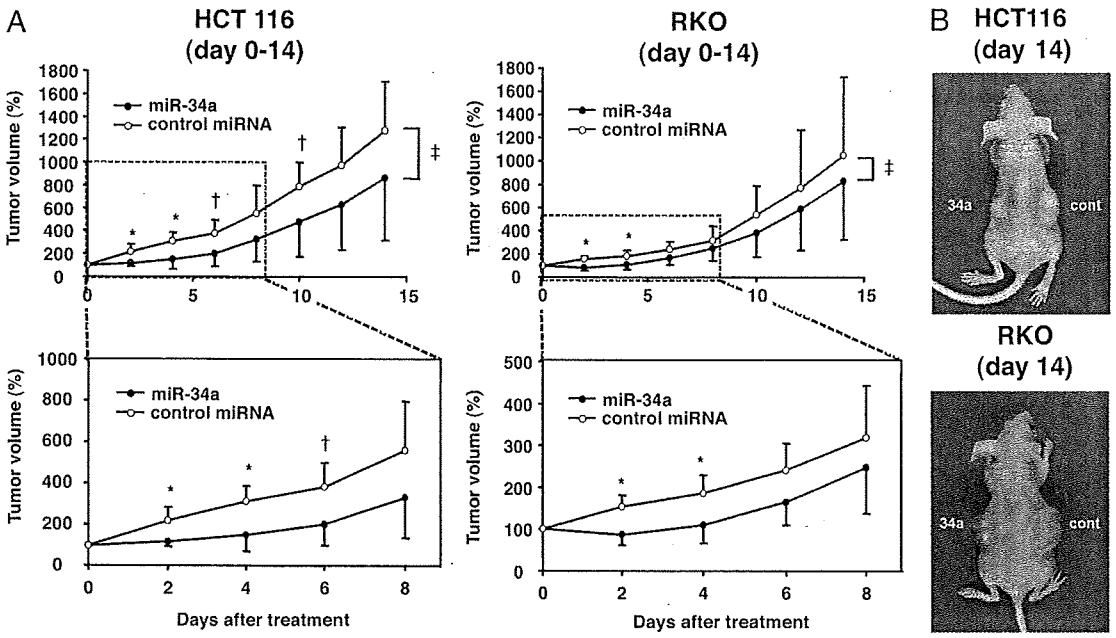

Fig. 3. Administration of *miR-34a* with atelocollagen suppresses tumor cell growth *in vivo*. (*A*) Upper graphs are growth curves of HCT 116 and RKO tumors after transplantation into nude mice with *miR-34a*/atelocollagen or control miRNA/atelocollagen complexes. The volume of the tumors derived from both cell lines at day 0, which was when control miRNA (open circles) and *miR-34a* (filled circles) treatment was performed, were set as 100%, and relative tumor volume was evaluated at 2-day intervals for 14 days and is plotted as the percentage relative to day 0. Lower graphs are enlarged images of the growth curves of tumors during the first 8 days after *miR-34a* administration. The data at each time point are expressed as mean values of 8 tumors in each experimental group with standard deviations. Note the significant suppression of tumor growth on days 2, 4, 6, and 10 for HCT 116 tumors, and on days 2 and 4 for RKO tumors (*, $P < 0.005$; †, $P < 0.05$). Significant differences (‡, $P < 0.05$) in the averaged tumor volumes were also observed in HCT 116 and RKO tumors between *mir-34a*- and control miRNA-administered tumors throughout the entire experimental period by adopting the linear mixed effect model (34). (*B*) Photographs illustrating representative features of mouse tumors derived from HCT 116 and RKO cells 14 days after treatment with control miRNA (cont) or *miR-34a* (34a).

observed in the triple knockout cells (23–25). This phenotype resembles the results obtained in our current study with *miR-34a* introduction in colon cancer cells.

Among the E2F family, E2F-3 seems to be a strong candidate for the *miR-34a* targets. Because E2F-3 is reported to be a regulator for E2F-1 gene expression at the transcriptional level (26), repression of other E2F family proteins might thus occur as a subsequent event by *miR-34a* overexpression. Activation of the p53 pathway could be caused as a consequence of the repression of the E2F family members as in the case of fibroblast with triple knockout of *E2f1–E2f3* (23–25) as described above. A positive feedback loop through the p53 pathway for *miR-34a* could be another important molecular basis for its transcriptional control, explaining the time-dependent increment in *miR-34a* induction in p53 wild-type colon cancer cells upon continuous exposure to ADR (Fig. 1*A*).

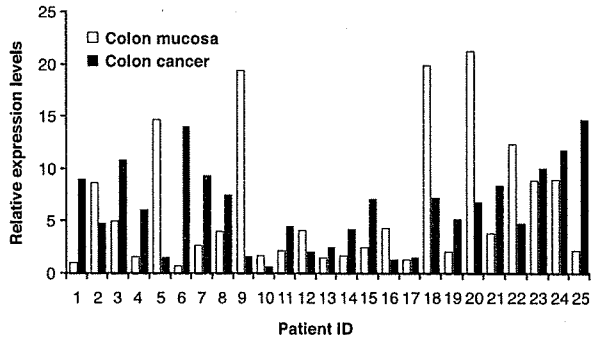

Fig. 4. Down-regulation of *miR-34a* expression in human colon cancer specimens. Quantitative real-time RT-PCR for *miR-34a* was carried out by using 25 surgical specimens of human colon cancer (filled bars) and paired noncancerous counterpart (open bars). The relative expression levels of *miR-34a* were calculated as described in Fig. 1.

It is also important to note that introduction of *miR-34a* represses cell proliferation of p53-knockout HCT 116 and other colon cancer cell lines with mutant p53 (SI Fig. 5). This observation indicates that enforced induction of exogenous *miR-34a* causes cell growth arrest in a p53-independent manner. The down-regulation of E2F family members, possibly through down-regulation of E2F-3 by overexpression of *miR-34a*, appears to be a key event for the induction of cellular senescence. Maehara *et al.* (27), indeed, recently revealed that reduction of E2F/DP activity induces senescence-like phenotypes in human cancer cells. Introduction of *miR-34a* also caused the up-regulation of the *HBP1* gene (SI Table 4), which is associated with oncogenic RAS-induced premature senescence (28). Thus, *miR-34a*-mediated modulation of several signaling pathways, including E2F- and RAS-related pathways, would collectively and effectively contribute to the induction of senescence-like phenotypes in human colon cancer cells.

Tumor cell growth in nude mice was significantly inhibited for 4–6 days after administration of *miR-34a*/atelocollagen complexes, but the suppressive effect was less prominent at later time points. Because complexed *miRNA* with atelocollagen is expected to stay stable for ≈1 week in this system (17), repeated injections of *miR-34a*/atelocollagen complexes may be required to exert tumor suppressive effects more efficiently and continuously.

Finally, it is of great interest to note that approximately one-third of human colon cancer specimens revealed down-regulation of the *miR-34a* expression. Similarly, quite recently, *miR-34a* was reported to be down-regulated in human primary

neuroblastomas with heterozygous deletion of chromosome 1p36, in which *miR-34a* resides (29). Because the same genomic region is also frequently deleted in colon cancers (30), down-regulation of *miR-34a* could be associated with the deletion of chromosome 1p36. Furthermore, deletions or mutations of the *p53* gene are also suggested to be causative genetic events underlying the down-regulation of *miR-34a* because its induction is tightly associated with p53 status (Fig. 1*B*). We indeed observed p53 mutations and chromosomal losses of 17p, including the *p53* locus, in some of the colon cancer specimens that showed down-regulation of *miR-34a* (unpublished observations). Epigenetic inactivation of *miR-34a* should also be considered as an underlying mechanism. Unexpectedly, we also observed that one-third of colon cancer cases showed up-regulation of *miR-34a*. There may be alternative mechanisms that remain to be identified in the regulation of *miR-34a*.

To conclude, the present demonstration of previously uncharacterized biological functions of *miR-34a*, with the ability to control cell proliferation and induce senescence-like changes in cancer cells, points to its significance as a unique type of tumor suppressor in colon cancer development.

Materials and Methods

Human Colon Cancer Cell Lines and ADR Treatment. The human colon cancer cell line, HCT 116, and the isogenic HCT 116 $p53^{-/-}$ cells (14) were kindly provided by Bert Vogelstein (The Johns Hopkins University, Baltimore, MD). Other human colon cancer cell lines, such as LoVo, RKO, DLD1, and HT29, were obtained from the American Type Culture Collection (Manassas, VA). DLD1 and HT29 cells are reported to harbor missense mutations in the *p53* gene at exon 7 (Ser241Phe) and exon 8 (Arg273His), respectively (31). HCT 116, HCT 116 $p53^{+/-}$, and HT29 cells were maintained in McCoy's 5A medium; and LoVo, RKO, and DLD1 cells were maintained in Ham's F12K medium, Dulbecco's modified Eagle's medium, and RPMI medium 1640, respectively. All media were supplemented with 10% FBS, 50 units/ml penicillin and 50 μg/ml streptomycin. The cells were routinely incubated at 37°C in a humidified atmosphere with 5% CO_2.

ADR was purchased from Sigma–Aldrich (St. Louis, MO). For isolation of total RNA and protein samples from various colon cancer cell lines, cells were seeded at 1.5×10^6 cells per 100-mm dish and treated with ADR at a concentration of 100 ng/ml for 16 h.

For the time course experiment of ADR treatment, HCT 116 cells were seeded at 6×10^5 cells per 60-mm dish and then incubated afterward with or without ADR in the culture medium. Cells were collected and subjected to extraction of total RNA and protein at 0, 1, 2, 4, 8, 12, 24, and 48 h thereafter.

Isolation of miRNA and Quantitative Real-Time RT-PCR Analysis. Total RNA, including miRNA, was extracted from the cells by using a mirVana miRNA Isolation Kit (Ambion, Austin, TX) according to the manufacturer's instructions and quantified with a NanoDrop spectrophotometer (NanoDrop Technologies, Wilmington, DE). cDNA was synthesized from 10 ng of total RNA by using a High Capacity cDNA Archive kit (Applied Biosystems, Foster City, CA), and the expression levels of 157 mature miRNA species were quantified by using a TaqMan MicroRNA Assays Human Panel (Applied Biosystems). Real-time RT-PCR was performed by using the Applied Biosystems 7300 Sequence Detection system (Applied Biosystems), the expression of each miRNA was defined from the threshold cycle (Ct), and relative expression levels were calculated by using the $2^{-\Delta\Delta Ct}$ method (32) after normalization with reference to expression of U6 small nuclear RNA.

Transient Transfection of Cells with *miR-34a* and Cell Proliferation Assay. HCT 116 and RKO cells were seeded at a density of 1.0×10^4 cells in 24-well tissue culture plates 24 h before transfection with 5 nM of either *miR-34a* (Ambion) or nontargeting control miRNA (control miRNA; Ambion) by using HiPerfect transfection reagents (Qiagen, Valencia, CA). The transfection efficiency under the conditions we adopted in this study was estimated to be close to 100% according to our observations made by using a fluorescence-labeled double-stranded short interference RNA. After transfection, cells were harvested and counted every day for 4 days. The average number of cells was determined at each time point in triplicate.

Microarray Analysis. Comprehensive gene-expression analysis of HCT 116 and RKO cells transfected with *miR-34a* or control miRNA was carried out by using the Whole Human Genome (4×44K) Oligo Microarray system (Agilent Technologies). Cells, seeded at 5×10^4 cells per ml in six-well tissue culture plates, were transfected with *miR-34a* or control miRNA as described above and propagated for 3 days. Total RNAs were isolated with an RNeasy column (Qiagen), and Cy3-labeled cRNA was prepared with an Agilent One Color Spike Mix Kit (Agilent Technologies) and then hybridized by using a Gene Expression Hybridization Kit (Agilent Technologies) at 65°C for 17 h. Signal intensity was calculated from digitized images captured by Laser Scanner (Agilent Technologies), and data analysis was performed by using GeneSpring GX software (Agilent Technologies).

Immunoblot Analysis. At day 3 after transfection with *miR-34a* or control miRNA, whole cell lysate was prepared in a lysis buffer (50 mM Tris·HCl, pH 7.4/150 mM NaCl/1% Triton X-100) with a protease inhibitor mixture (Complete Mini; Roche, Indianapolis, IN). Proteins were electrophoresed on a 5–20% linear gradient Tris·HCl-ready gels (Bio-Rad, Hercules, CA) and transferred to polyvinylidene fluoride membranes (Immobiron-P; Millipore, Billerica, MA). Blots were blocked with 3% nonfat dry milk in TBS-T (Tris-buffered saline/0.1% Tween-20, pH 7.4) at room temperature for 30 min. For primary antibodies, we used mouse anti-p53 mAb (1:200, DO-1; Santa Cruz Biotechnology, Santa Cruz, CA), mouse anti-p21 mAb (1:2,000, DCS60; Cell Signaling Technology, Beverly, MA), mouse anti-α-tubulin mAb (1:5,000, DM1A, ICN Biomedicals, Irvine, CA), mouse PARP mAb (1:1,000, C-2–10, Oncogene Research Products, San Diego, CA), mouse anti-caspase-3 mAb (1:1,000, 3G2; Cell Signaling Technology), rabbit anti-E2F-1 polyclonal antibody (pAb) (1:500, C-20; Santa Cruz Biotechnology), rabbit anti-E2F-2 pAb (1:1,000, C-20; Santa Cruz Biotechnology), and rabbit anti-E2F-3 pAb (1:1,000, C-18; Santa Cruz Biotechnology). Horseradish peroxidase-conjugated antibodies against mouse IgG or rabbit IgG (1:5,000–10,000, NA9310V; Amersham Biosciences, Piscataway, NJ) were used as secondary antibodies. Immunoreactive bands on the blots were visualized with enhanced chemiluminescence substrates (Immobilon Western; Millipore).

SA-β-Gal Staining. At day 4 after transfection with *miR-34a* or control miRNA, HCT 116 and RKO cells were fixed and stained by using an SA-β-gal kit (Cell Signaling Technology) according to the manufacturer's instructions.

Human Tumor Xenograft Model and Administration of *miR-34a*/Atelocollagen Complexes. Animal experimental protocols were approved by our institute's Committee for Ethics in Animal Experimentation, and the experiments were conducted in accordance with the guidelines for Animal Experiments of the National Cancer Center. HCT 116 or RKO cells were inoculated with 5×10^6 cells per site bilaterally on the backs of female athymic nude mice aged 6 weeks (Charles River Laboratories,

Wilmington, MA). Tumor size was monitored by measuring the length and width with calipers, and volumes were calculated with the formula: $(L \times W^2) \times 0.5$, where L is length and W is width of each tumor.

Atelocollagen was pretreated with pepsin to remove the telopeptides, which confer most of the collagen's antigenicity (33), and complexes of *miR-34a* (Ambion) and control miRNA (Ambion) with atelocollagen were prepared as described in refs. 15–17. The *miR-34a* and control miRNA (15 μg) with 0.5% atelocollagen in a 200-μl volume were administered into the s.c. spaces around the tumors when they had reached a volume of 50–100 mm^3 at day 6 after inoculation. The volume of each tumor at the point of *miR-34a* or control miRNA administration was set at 100%, and the relative tumor volumes at each time point was evaluated every other day from days 2 to 14.

Immunohistochemistry. Tumors were fixed in 10% neutralized formalin and embedded in paraffin blocks. Sections (4 μm) were prepared for hematoxylin/eosin staining and also for immunohistochemical examination. After deparaffinization and rehydration, antigen retrieval was performed by microwave irradiation at 600 W for 10 min in 10 mM citrate buffer (pH 6.0). Tissue sections were incubated with rabbit anti-Ki67 polyclonal antibody (pAb) (1:1,000; Novocastra Laboratories, Newcastle, U.K.), mouse anti-p21 mAb (1:100) and rabbit anti-cleaved caspase-3 mAb (1:200, 5A1; Cell Signaling Technology). The sections were then incubated with goat biotinylated anti-rabbit IgG antibody and goat biotinylated anti-mouse IgG antibody (1:200; Vector Laboratories, Burlingame, CA). Immunoreactive signals were visualized by using 3,3′-diaminobenzidine tetrahydrochloride solution, and the nuclei were counterstained with hematoxylin.

Human Colon Cancer Samples. Primary human colon cancers and paired noncancerous normal colon samples were obtained from 25 patients treated at the National Cancer Center Hospital, Tokyo, with documented informed consent in each case. Samples were frozen in liquid nitrogen and stored at −80°C until use. Total RNA was isolated from frozen samples by using TRIzol reagent (Invitrogen), and then quantitative real-time RT-PCR for *miR-34a* and U6 small nuclear RNA was performed as described above. The relative expression level of *miR-34a* in each sample was calculated and quantified by using the $2^{-\Delta\Delta Ct}$ method after normalization for expression of U6 small nuclear RNA as described above.

Statistical Analysis. The Mann–Whitney U test was used to test for statistical significance of differences in tumor volumes at each time point after administration of *miR-34a* and control miRNA. We also used linear mixed effect models (34) to evaluate the differences in averaged volumes of tumors throughout the entire experimental period between the two experimental groups, namely *miR-34a*- and control miRNA-administered groups. $P < 0.05$ was considered significant.

Note. During the process of submitting our manuscript, three related papers by Raver-Shapira *et al.* (35), Chang *et al.* (36), and He *et al.* (37) were published.

We thank Dr. Bert Vogelstein for providing the HCT 116 and HCT 116 p53$^{-/-}$ cells; Dr. Takahiro Ochiya (National Cancer Center Research Institute) and Dr. Fumitaka Takeshita (National Cancer Center Research Institute) for providing us with atelocollagen and for helpful discussion; and Dr. Kenichi Yoshimura for his kind help in statistical analysis. This work was supported in part by a Grant-in-Aid for Cancer Research for the Third-Term Comprehensive 10-Year Strategy for Cancer Control from the Ministry of Health, Labour and Welfare of Japan and by Research Grant 06-016 of the Sankyo Foundation of Life Science. M.I. is a recipient of the Research Resident Fellowship from the Foundation for Promotion of Cancer Research in Japan.

1. Lengauer C, Kinzler KW, Vogelstein B (1998) *Nature* 396:643–649.
2. Baylin SB, Ohm JE (2006) *Nat Rev Cancer* 6:107–116.
3. Esteller M (2007) *Nat Rev Genet* 8:286–298.
4. Tomaru Y, Hayashizaki Y (2006) *Cancer Sci* 97:1285–1290.
5. Bartel DP (2004) *Cell* 116:281–297.
6. Alvarez-Garcia I, Miska EA (2005) *Development (Cambridge, UK)* 132:4653–4662.
7. Calin GA, Croce CM (2006) *Nat Rev Cancer* 6:857–866.
8. Lu J, Getz G, Miska EA, Alvarez-Saavedra E, Lamb J, Peck D, Sweet-Cordero A, Ebert BL, Mak RH, Ferrando AA, *et al.* (2005) *Nature* 435:834–838.
9. Volinia S, Calin GA, Liu CG, Ambs S, Cimmino A, Petrocca F, Visone R, Iorio M, Roldo C, Ferracin M, *et al.* (2006) *Proc Natl Acad Sci USA* 103:2257–2261.
10. Calin GA, Ferracin M, Cimmino A, Di Leva G, Shimizu M, Wojcik SE, Iorio MV, Visone R, Sever NI, Fabbri M, *et al.* (2005) *N Engl J Med* 353:1793–1801.
11. Fukuda H, Sugimura T, Nagao M, Nakagama H (2001) *Biochim Biophys Acta* 1528:152–158.
12. Caudy AA, Ketting RF, Hammond SM, Denli AM, Bathoorn AM, Tops BB, Silva JM, Myers MM, Hannon GJ, Plasterk RH (2003) *Nature* 425:411–414.
13. Tsuchiya N, Ochiai M, Nakashima K, Ubagai T, Sugimura T, Nakagama H (2007) *Cancer Res*, in press.
14. Bunz F, Dutriaux A, Lengauer C, Waldman T, Zhou S, Brown JP, Sedivy JM, Kinzler KW, Vogelstein B (1998) *Science* 282:1497–1501.
15. Minakuchi Y, Takeshita F, Kosaka N, Sasaki H, Yamamoto Y, Kouno M, Honma K, Nagahara S, Hanai K, Sano A, *et al.* (2004) *Nucleic Acids Res* 32:e109.
16. Takeshita F, Minakuchi Y, Nagahara S, Honma K, Sasaki H, Hirai K, Teratani T, Namatame N, Yamamoto Y, Hanai K, *et al.* (2005) *Proc Natl Acad Sci USA* 102:12177–12182.
17. Takei Y, Kadomatsu K, Yuzawa Y, Matsuo S, Muramatsu T (2004) *Cancer Res* 64:3365–3370.
18. Bunz F, Hwang PM, Torrance C, Waldman T, Zhang Y, Dillehay L, Williams J, Lengauer C, Kinzler KW, Vogelstein B (1999) *J Clin Invest* 104:263–269.
19. Marsit CJ, Eddy K, Kelsey KT (2006) *Cancer Res* 66:10843–10848.
20. Pogribny IP, Tryndyak VP, Boyko A, Rodriguez-Juarez R, Beland FA, Kovalchuk O (2007) *Mutat Res* 619:30–37.
21. Tsantoulis PK, Gorgoulis VG (2005) *Eur J Cancer* 41:2403–2414.
22. Leone G, Sears R, Huang E, Rempel R, Nuckolls F, Park CH, Giangrande P, Wu L, Saavedra HI, Field SJ, *et al.* (2001) *Mol Cell* 8:105–113.
23. Wu L, Timmers C, Maiti B, Saavedra HI, Sang L, Chong GT, Nuckolls F, Giangrande P, Wright FA, Field SJ, *et al.* (2001) *Nature* 414:457–462.
24. Sharma N, Timmers C, Trikha P, Saavedra HI, Obery A, Leone G (2006) *J Biol Chem* 281:36124–36131.
25. Timmers C, Sharma N, Opavsky R, Maiti B, Wu L, Wu J, Orringer D, Trikha P, Saavedra HI, Leone G (2007) *Mol Cell Biol* 27:65–78.
26. Johnson DG, Ohtani K, Nevins JR (1994) *Genes Dev* 8:1514–1525.
27. Machara K, Yamakoshi K, Ohtani N, Kubo Y, Takahashi A, Arase S, Jones N, Hara E (2005) *J Cell Biol* 168:553–560.
28. Zhang X, Kim J, Ruthazer R, McDevitt MA, Wazer DE, Paulson KE, Yee AS (2006) *Mol Cell Biol* 26:8252–8266.
29. Welch C, Chen Y, Stallings RL (2007) *Oncogene* 26:5017–5022.
30. Martens F, Johansson B, Hoglund M, Mitelman F (1997) *Cancer Res* 57:2765–2780.
31. Rodrigues NR, Rowan A, Smith ME, Kerr IB, Bodmer WF, Gannon JV, Lane DP (1990) *Proc Natl Acad Sci USA* 87:7555–7559.
32. Livak KJ, Schmittgen TD (2001) *Methods* 25:402–408.
33. Ochiya T, Takahama Y, Nagahara S, Sumita Y, Hisada A, Itoh H, Nagai Y, Terada M (1999) *Nat Med* 5:707–710.
34. Laird NM, Ware JH (1982) *Biometrics* 38:963–974.
35. Raver-Shapira N, Marciano E, Meiri E, Spector Y, Rosenfeld N, Moskovits N, Bentwich Z, Oren M (2007) *Mol Cell* 26:731–743.
36. Chang TC, Wentzel EA, Kent OA, Ramachandran K, Mullendore M, Lee KH, Feldmann G, Yamakuchi M, Ferlito M, Lowenstein CJ, *et al.* (2007) *Mol Cell* 26:745–752.
37. He L, He X, Lim LP, de Stanchina E, Xuan Z, Liang Y, Xue W, Zender L, Magnus J, Ridzon D, *et al.* (2007) *Nature* 447:1130–1134.

SND1, a Component of RNA-Induced Silencing Complex, Is Up-regulated in Human Colon Cancers and Implicated in Early Stage Colon Carcinogenesis

Naoto Tsuchiya, Masako Ochiai, Katsuhiko Nakashima, Tsuneyuki Ubagai, Takashi Sugimura, and Hitoshi Nakagama

Biochemistry Division, National Cancer Center Research Institute, 5-1-1 Tsukiji, Chuo-ku, Tokyo, Japan

Abstract

Colon cancers have been shown to develop after accumulation of multiple genetic and epigenetic alterations with changes in global gene expression profiles, contributing to the establishment of widely diverse phenotypes. Transcriptional and posttranscriptional regulation of gene expression by small RNA species, such as the small interfering RNA and microRNA and the RNA-induced silencing complex (RISC), is currently drawing major interest with regard to cancer development. SND1, also called Tudor-SN and p100 and recently reported to be a component of RISC, is among the list of highly expressed genes in human colon cancers. In the present study, we showed remarkable up-regulation of *SND1* mRNA in human colon cancer tissues, even in early-stage lesions, and also in colon cancer cell lines. When mouse Snd1 was stably overexpressed in IEC6 rat intestinal epithelial cells, contact inhibition was lost and cell growth was promoted, even after the cells became confluent. Intriguingly, IEC6 cells with high levels of Snd1 also showed an altered distribution of E-cadherin from the cell membrane to the cytoplasm, suggesting loss of cellular polarity. Furthermore, the adenomatous polyposis coli (Apc) protein was coincidentally down-regulated, with no significant changes in the *Apc* mRNA level. Immunohistochemical analysis using chemically induced colonic lesions developed in rats revealed overexpression of Snd1 not only in colon cancers but also in aberrant crypt foci, putative precancerous lesions of the colon. Up-regulation of SND1 may thus occur at a very early stage in colon carcinogenesis and contribute to the posttranscriptional regulation of key players in colon cancer development, including APC and β-catenin. [Cancer Res 2007;67(19):9568–76]

Introduction

Altered gene expression, as a consequence of genetic alterations and/or epigenetic changes in the methylation status at promoter CpG sites, is a characteristic of cancers (1, 2). Expression of genes is regulated at both transcriptional and posttranscriptional levels, and differential gene expression profiles confer a wide range of diverse phenotypes in cancer cells. Dysregulation of various transcription factors is well known to be a causative event involved in malignant transformation, for example, with functional inactivation or intragenic mutation of p53 (3), and gene amplification or overexpression of c-myc (4).

Recently, posttranscriptional regulation, especially translational control, of gene expression has become a major interest in the field of cancer research, because accumulating evidence strongly suggests its biological relevance for cancer development and progression (5). Some oncogenes and tumor suppressor genes, including c-myc (6), Mdm-2 (7), and p53 (8), have been shown to be regulated at the translational level. Overexpression of the translation initiation factor eIF4E promotes malignant transformation of normal fibroblasts (9) and cooperates with c-Myc to drive B-cell lymphomatogenesis in eIF4E transgenic mice (10). Very recently, microRNA, another important factor for both transcriptional and translational gene expression regulation (11, 12), has been revealed to have a substantial effect on human carcinogenesis (13), and there are many examples of genetic alterations in microRNA gene loci, including deletions, amplifications, and mutations (14–16).

SND1, also known as Tudor-SN and p100, is a highly conserved protein from yeasts to humans, but its biological functions remain to be fully elucidated. The protein has five repeated staphylococcal nuclease homology domains and a Tudor-homology domain suggested to act as interaction platforms for nucleic acids and proteins, respectively (17). The protein was first identified as a coactivator of the EBV nuclear antigen 2 (18) and was later shown to interact with the oncogene product c-Myb (19). It is thus a transcriptional coactivator (19–21).

We have identified a mouse homologue of SND1 as a single-stranded cytosine-rich DNA binding protein, which binds to the d(CTGCC)n sequence derived from mouse minisatellite Pc-1 with high affinity (22), but not to a complementary guanine-rich repetitive sequence d(GGCAG)n and its double-stranded form (23). Caudy et al. recently reported that SND1 is one of the components of the RNA-induced silencing complex (RISC), and disruption of SND1 in *C. elegance* was shown to cause disruption of small interfering RNA-induced gene silencing (24). In addition, SND1 is among the top five genes up-regulated in human colon adenocarcinomas, as assessed using oligonucleotide microarrays (25). Although biological functions of SND1 still remain largely elusive, the recent intriguing findings suggest an involvement of SND1 as a key player in the regulation of gene expression at both transcriptional and posttranscriptional levels through direct binding to RNA in some sequence-specific manner. Our working hypothesis is that overexpression of SND1, therefore, has a substantial effect on carcinogenesis.

In the present study, we investigated the possible involvement of SND1, a component of RISC, in colon carcinogenesis. We first conducted expression analysis of *SND1* mRNA in human colon

Note: Supplementary data for this article are available at Cancer Research Online (http://cancerres.aacrjournals.org/).

Present address for K. Nakashima: Department of Biochemistry and Molecular Pharmacology, University of Massachusetts Medical School, 364 Plantation Street, Worcester, MA.

Requests for reprints: Hitoshi Nakagama, Biochemistry Division, National Cancer Center Research Institute, 5-1-1 Tsukiji, Chuo-ku, Tokyo, 104-0045, Japan. Phone: 81-3-3547-5239; Fax: 81-3-3542-2530; E-mail: hnakagam@gan2.res.ncc.go.jp.

doi:10.1158/0008-5472.CAN-06-2707

cancer tissues and several colon cancer cell lines and found marked up-regulation of *SND1* mRNA in colon cancer cells. Immunohistochemical analysis using various stages of colonic lesions induced in rats by chemical carcinogens revealed overexpression of Snd1 in precancerous lesions of the colon even before the appearance of β-catenin accumulation. Intriguingly, introducing a recombinant HA-tagged mouse Snd1 protein caused down-regulation of the adenomatous polyposis coli (Apc) protein and translocation of E-cadherin from the cell membrane to the cytoplasm, leading to loss of contact inhibition and cellular polarity. A possible involvement of SND1 in early stages of colon carcinogenesis through its novel function as a posttranscriptional regulator is proposed.

Materials and Methods

Surgical tissue specimens, cell lines, and antibodies. Paired surgical specimens of primary human colon cancers and surrounding noncancerous counterparts of the colon were obtained from 32 patients treated at the National Cancer Center Hospital, Tokyo, Japan, with documented informed consent in each case. Samples were frozen in liquid nitrogen and stored at −80°C until use. Clinicopathologic staging of cancers was done according to the criteria approved by the American Joint Committee on Cancer. Nine cases were diagnosed as stage II, 12 cases as stage III, and 11 cases as stage IV. Ten human colon cancer cell lines were maintained in the complete growth medium recommended by the American Type Culture Collection. Antibodies used in this study were rabbit anti-HA and anti–α-tubulin antibodies purchased from Sigma, rat monoclonal anti-HA antibody from Roche, anti-E-cadherin, anti–β-catenin, p120 catenin antibodies from BD Bioscience, anti-APC antibodies, C-20 and Ab-1, from Santa Cruz Biotech, Inc. and Chemicon, respectively. For secondary antibodies, Alexa-labeled anti-rabbit and mouse antibodies were from Invitrogen Corp., horseradish peroxidase–conjugated anti-rabbit and mouse IgG is from GE Health Bio-Science, and HRP-conjugated anti-rat IgG is from Sigma. A rabbit polyclonal anti-SND1 antibody was raised by immunizing rabbits using purified recombinant thioredoxin–tagged Snd1 protein expressed in *Escherichia coli*. Anti-SND1 antiserum was purified by affinity chromatography using CNBr-sepharose (GE Healthcare Bio-Science) cross-linked with glutathione *S*-transferase–tagged Snd1 protein.

Quantitative real-time reverse transcription-PCR analysis. Total RNA was isolated from ~30 mg of surgical samples and 5×10^6 culture cells using Trizol reagent (Invitrogen). After treatment with DNase I, 2 μg of aliquots of RNA were subjected to cDNA synthesis using SuperScript II reverse transcriptase (Invitrogen) and oligo$(dT)_{12\text{-}18}$ as a primer. Primer sequences for reverse transcription-PCR (RT-PCR) amplification of the human *SND1* mRNA were 5′-GTGGACAGCGTAGTTCGGGA-3′ (forward) and 5′-CCCACGAGACATTTCCACACAC-3′ (reverse) designed from nucleotide sequences in exons 17 and 22, respectively. Quantitative RT-PCR was carried out in a total of 25 μL of reaction mixture by a SmartCycler (Takara) using SYBR Green reagent and *Takara Ex* Taq (R-PCR version 2.1, Takara) and analyzed with SmartCycler software version 1.0 following the manufacturer's instructions. For reference, mRNA levels of β-actin were amplified using a primer set, 5′-GACTTCGAGCAAGAGATGGC-3′ (forward) and 5′-AGGAAGGAAGGCTGGAAGAG-3′ (reverse), as described previously (26). Relative amounts of *SND1* mRNA were calculated by the division of the copy number of *SND1* transcripts with those of *β-actin*. Statistical analyses were done using JMP 6.0 software (JMP Japan).

Establishment of recombinant Snd1-expressing rat intestinal epithelial cells, IEC6. *Snd1* cDNA derived from mouse NIH3T3 cells (23) was subcloned into a pEF6-HA vector by the standard method (27). The plasmid, pcEF6-HA-Snd1 or pEF6-HA (vector control), was introduced in the IEC6 cells using LipofectAMINE 2000 (Invitrogen) according to the manufacturer's instructions. Transfected cells were grown in the selection medium composed of complete DMEM containing 5% fetal bovine serum (FBS), 10 μg/mL insulin, and 3 μg/mL blasticidin, and stable clones were isolated. Expression of HA-Snd1 in transfected cells was confirmed by immunoblot analysis and/or immunostaining of the cells using anti-HA antibody.

Cell growth assay and immunocytochemistry. IEC6 cells stably expressing the exogenously introduced HA-Snd1, and vector-transfected IEC6 cells were seeded on 24-well plates at a density of 2.5×10^4 cells/mL (0.5 mL/well) and grown in complete growth medium as described above for the indicated number of days. Cells were collected and counted at each time point. Cells, seeded on glass-bottomed plates, were fixed in cold methanol and blocked in 5% bovine serum albumin/PBS for 60 min at room temperature. Fixed cells were incubated in blocking buffer containing the first antibodies of anti-HA or anti–E-cadherin for 60 min, and then incubated with the secondary antibody for 60 min. After washing with PBS containing Hoechst 33258, cells were subjected to fluorescent microscopic observation using an Axiovert 200 fluorescence microscope (Carl Zeiss).

Immunoblot analysis. A series of IEC-Snd and IEC-vector cells were lysed in Laemmli's SDS sample buffer (28), then subjected to immunoblot analysis. The membrane was immersed in blocking buffer consisting of 10% dried milk/TBS-0.05% Tween 20 for 60 min at room temperature. The membrane was then incubated with the primary antibodies for 60 min, then incubated with the secondary antibodies, and detected by enhanced chemiluminescence plus reagent (GE Healthcare Bio-Science).

Induction of precancerous colon lesions *in vivo*. Five-week old F344 rats were purchased from CLEA Japan and housed in a ventilated, temperature-controlled room at 25°C with a 12-h light/dark cycle. Two carcinogenic chemicals, azoxymethane and 2-amino-1-methyl-6-phenylimidazo[4,5-*b*]pyridine (PhIP), were both purchased from the Nard Institute and used for the induction of colonic lesions. One group of rats was injected with azoxymethane (15 mg/kg body weight) weekly for 2 weeks, and fed continuously with a basal diet (AIN-93G; Dyets, Inc.). Another group of rats was fed a diet containing 400 ppm of PhIP following our intermittent administration protocol, as described previously (29). Animals treated with azoxymethane and PhIP were sacrificed at weeks 10 and 32, respectively, and subjected to histologic analysis. Aberrant crypt foci (ACF), putative precancerous lesions of the colon, were dissected, as detailed elsewhere (30), and embedded in paraffin. Serial paraffin sections of ACF were prepared and stained with H&E to evaluate the histologic grade of ACF, namely nondysplastic ACF and dysplastic ACF, according to their cytologic and structural abnormalities, as described previously (31). Animal experiments in the present study were approved by the Institutional Animal Care and Use Committee at the National Cancer Center.

Immunohistochemical analysis of Snd1 in colon tumors and ACF. Paraffin sections of colon cancers and ACF induced in the rat colon by azoxymethane and PhIP were immunostained with a polyclonal anti-SND1 antibody (α-SND1) and anti–β-catenin antibody. Sections were deparaffinized with xylene and rehydrated with graded ethanol. Antigen retrieval was carried out by autoclaving for 15 min in target retrieval solution (DacoCytomation) for Snd1 and in 10 mmol/L citrate buffer (pH 6.0) for β-catenin. Immunohistochemical staining was done by the avidin-biotin complex method (ABC) using the Vectastain Elite ABC system (Vector Laboratories) as described previously (30). α-SND1 was used at a concentration of 0.2 μg/mL. Biotinylated goat anti-rabbit IgG (Vector Laboratories) was used as a secondary antibody for both at a dilution of 1:200.

Results

Up-regulation of *SND1* mRNA expression in human colon cancers. As shown in Fig. 1*A*, quantitative RT-PCR analysis revealed marked up-regulation of *SND1* mRNA in most human cancer tissues examined, and 28 of 32 colon cancer cases showed 2-fold or greater increase compared with their noncancerous counterparts. The expression levels of *SND1* mRNA in colon cancer tissues normalized to that of the *β-actin* transcript (*SND1* mRNA copy number/*β-actin* mRNA copy number) was 0.033 ± 0.015, which is ~5-fold higher compared with those of normal counterparts, 0.007 ± 0.003. Statistical analysis confirmed a highly significant up-regulation of *SND1* in colon cancers (paired *t* test,

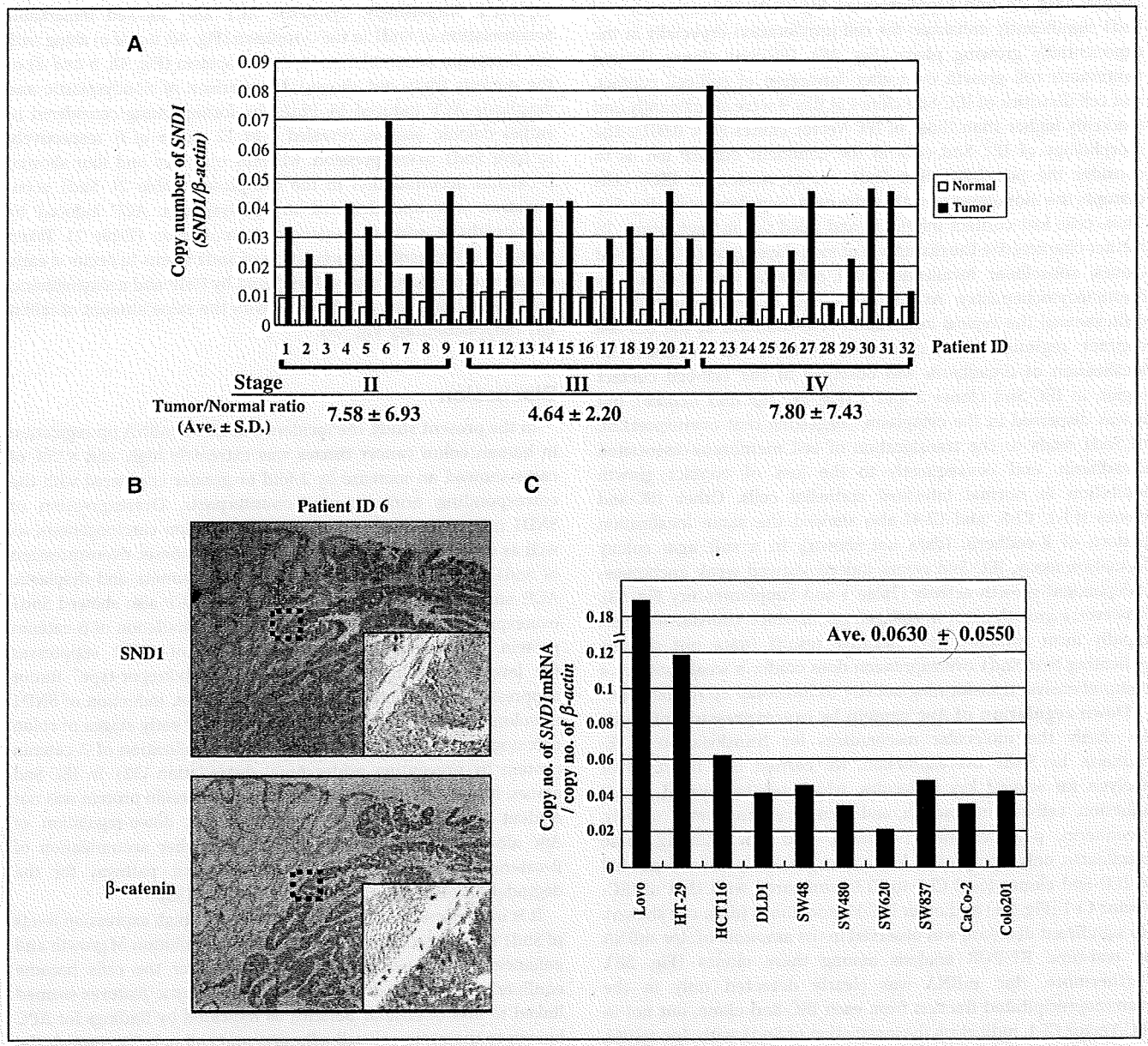

Figure 1. *SND1* mRNA is highly up-regulated in colon cancer cells. *A,* surgical specimens of 32 human colorectal cancers were subjected to quantitative real-time RT-PCR. Twenty-eight cases showed up-regulation of *SND1* mRNA by 2-fold or greater compared with their normal counterparts, and the remaining four cases (16, 23, 28, 32) also showed slight, but <2-fold, increase of the transcript. Stages II, III, and IV are patients 1 to 9, 10 to 21, and 22 to 32, respectively. The average fold changes between the tumor and normal counterpart in the total and each stage are indicated. A statistical analysis was carried out by paired *t* test. *B,* immunohistochemical analysis of human colon cancer tissues. Serial paraffin sections of colon tumors derived from patients 6, 22, 24, and 27 were examined immunohistochemically with anti-SND1 and anti–β-catenin antibodies. Representative results using tissue sections of patient 6 are shown. Subcellular localization of SND1 and β-catenin is indicated by enlarged images in the small boxes, and enlarged regions are marked by squares with a dotted line. Low and high magnifications are ×40 and ×100, respectively. *C,* expression levels of *SND1* mRNA in 10 human colon cancer cell lines were evaluated. All colon cancer cell lines show remarkably high copy numbers of the *SND1* transcript normalized by those of the *β-actin* transcript, ranging from 0.18 in Lovo to 0.021 in SW620.

$P < 0.0001$). No significant differences were observed in *SND1* expression levels among different clinicopathologic stages of cancer (Student's *t* test, $P > 0.2$). Cytoplasmic accumulation of SND1 protein was confirmed by immunohistochemical analysis using colon cancer tissues (Fig. 1*B*). High expression of *SND1* mRNA was also observed in all 10 human colon cancer cell lines examined (Fig. 1*C*). The average expression level of *SND1* mRNA in colon cancer cell lines, being 0.063 ± 0.045, was comparable with that detected in colon cancer tissues.

Expression of recombinant Snd1 leads to loss of contact inhibition and promotes cell proliferation in IEC6 cells. IEC6 cells were stably transfected with a construct encoding HA-tagged mouse Snd1, and five independent clones were established expressing much higher levels of total Snd1 protein (a series of IEC-Snd clones) compared with the vector-transfected cell clones (a series of IEC-Vector clones). The expression levels of HA-Snd1 and total Snd1 (endogenous Snd1 plus HA-Snd1) in IEC-Snd1 clones and IEC-Vector clones were confirmed by immunoblot

analysis (Fig. 2*A* and Supplementary Fig. S1*B*). Overexpression of Snd1 significantly enhanced the cell proliferation especially in the exponentially growing phase (Fig. 2*B*). IEC-Snd clones showed continuous cell growth even after formation of cell-cell contact, and cell densities of IEC-Snd clones at day 9 were significantly and markedly higher than those of IEC-Vector clones ($P < 0.001$). The morphology of IEC-Snd cells in the confluent culture led us to consider the possibility that Snd1 overexpression in IEC6 cells disrupts the monolayer growth of the cells (Supplementary Fig. S2). Thus, cells lost contact inhibition and piled up on each other. To further characterize the disruption of monolayer growth in IEC-Snd clones, subcellular localization of E-cadherin was analyzed by immunocytochemistry. As shown in Fig. 2*C*, vector-transfected cells showed the typical localization of E-cadherin at the cell-cell contact regions (IEC-vector Cl-1, *bottom*). In contrast, no localization of E-cadherin was observed at the cell-cell contact region in IEC-Snd clones 2 and 5 (Fig. 2*C, top and middle*), but it was dispersed in the cytoplasm, suggesting that overexpression of Snd1 leads to the translocation of cell membrane–associated E-cadherin, and consequently to the loss of contact growth inhibition in normal intestinal epithelial cells. Other IEC-Snd clones (Cl-1, Cl-3, and Cl-4) also showed the same localization pattern of E-cadherin (data not shown). In a soft agar colony formation assay, IEC-Snd clones indeed showed weak anchorage-independent growth activity (Table 1 and Supplementary Fig. S3). However, a growth assay in collagen gel, in which transformed cells rapidly form colonies, gave negative results (data not shown), indicating that Snd1 overexpression does confer a weak, but not a comprehensive, transforming activity to intestinal epithelial cells.

Down-regulation of Apc protein by overexpression of Snd1. To clarify the molecular mechanisms for translocation of E-cadherin by Snd1 overexpression, we carried out immunoblot analysis for several key molecules, which are implicated in cell adhesion, cell-cell interaction, and colon carcinogenesis, namely, E-cadherin, p120 catenin, β-catenin, and Apc. Among these candidates, only Apc protein levels were markedly down-regulated in IEC-Snd clones (Snd Cl-1 to Cl-5) compared with that of IEC-Vector Cl-1 (Fig. 3*A*) and other IEC-Vector clones (data not shown). No significant decrease was observed in the amounts of *Apc* mRNA by real-time RT-PCR analysis among these clones (Fig. 3*B*). Furthermore, *Apc* mRNA was clearly detected only in the immunoprecipitated fraction from each IEC-Snd clone, but not in IEC-Vector Cl-1, indicating the association of Snd1 with *Apc* mRNA in cells (Fig. 3*C*). The interaction of Snd1 with *APC* mRNA was also confirmed by transient expression of HA-Snd1 into HeLa cells (data not shown). This strongly suggests that the expression of the Apc protein could be regulated by some posttranscriptional mechanisms, neither by transcription nor by mRNA stability. Transient introduction of the human SND1 to HCT 116 and SW 48 colon cancer cell lines and HeLa cells, all of which express wild-type APC, also caused the down-regulation of the APC protein (Supplementary Fig. S4*A*) without significant changes in *APC* mRNA levels (Supplementary Fig. S4*B*).

Accumulation of Snd1 protein in ACF and colon tumors of rats. To gain further insight into the biological role of Snd1 in an *in vivo* setting, we investigated whether Snd1 is expressed in chemically induced colonic lesions induced in rats. Immunohistochemical analysis of Snd1 and β-catenin was carried out in colon cancers induced by azoxymethane or PhIP and in ACF. Colon cancers induced by azoxymethane (Fig. 4*A*) and PhIP (data not shown) showed accumulation of both β-catenin and Snd1, as expected. Surprisingly, dysplastic ACF also showed remarkable accumulation of Snd1 in the cytoplasm (Fig. 4*B, a and c*) along with the β-catenin accumulation in the cytoplasm (Fig. 4*B, b and d*) or the nucleus (data not shown). Comparison of nondysplastic and dysplastic ACF induced by PhIP, the former being considered as earlier colonic lesions, revealed 7 of 12 and 6 of 6, respectively, to have Snd1 overexpression, whereas only two and four showed β-catenin accumulation in the cytoplasm (Table 2). Snd1 accumulation was also detected in nondysplastic ACF induced by azoxymethane without β-catenin accumulation (Table 2). Taken together, cytoplasmic accumulation of Snd1 seems to occur at early stages in colon carcinogenesis induced by PhIP and azoxymethane. Positive staining was not detected with the same amount of rabbit IgG (Supplementary Fig. S5).

Discussion

In the present study, the incidence of *SND1* mRNA up-regulation in human colon cancer tissues was extremely high, and 87.5% of cases showed an increase by 2-fold or greater compared with the corresponding noncancerous counterparts. Overexpression of SND1 may have some significant role in colon carcinogenesis, as well as other tissues. In support of this hypothesis, overexpression of Snd1 was commonly observed in colon tumors and dysplastic ACF, and surprisingly, some nondysplastic ACF also showed Snd1 overexpression even before cytoplasmic accumulation of β-catenin protein. Considering that overexpression of SND1 suppresses the levels of APC protein, which is a "gatekeeper-type" tumor suppressor gene in colon cancer development, induction of SND1 in colonic epithelial cells could occur at very early stages of colon carcinogenesis. Loss of Apc leads to the stabilization of β-catenin protein by preventing proteasomal degradation (32). In IEC-Snd clones, however, a significant increase of β-catenin protein was not evident (data not shown), suggesting that down-regulation of Apc alone may not be enough for the further accumulation of β-catenin. Alternatively, an Apc-independent pathway for the degradation of β-catenin might be involved (33).

It is important to note that IEC6 cells with high expression levels of Snd1 manifested loss of cell-cell contact inhibition of growth and enhancement of cell proliferation even after the cells became confluent on culture dishes. These characteristic features seemed linked to loss of cellular polarity, as indicated by findings for APC known to maintain cell-cell adhesion and cell polarity through the regulation of localization of E-cadherin to the plasma membrane (34). Loss of cellular polarity and abnormal growth of cryptic epithelial cells are suspected to occur at the very beginning of intestinal carcinogenesis (35), as is also well represented in the case of *Apc*-disrupted mice (36). Collectively, functional activation of SND1 could be a novel molecular basis underlying the initial development of precancerous lesions in the colon.

We also noted that knockdown of SND1 by small interfering RNA did not cause significant up-regulation of APC protein level in several colon cancer cell lines, except SW48 cells, and did not inhibit cell proliferation. Down-regulation of SND1 alone may not be sufficient to increase the APC protein level in cancer cells or to overcome the aberrant cell proliferation of fully transformed cells, which harbor complex genetic and epigenetic changes, including those implicated in the *WNT* signaling pathway, *p53*, *K-RAS*, and *SMADs*. We further failed to detect the translocation of E-cadherin in both chemically induced precancerous lesions in the rat colon and human colon cancer tissues (data not shown). This might be

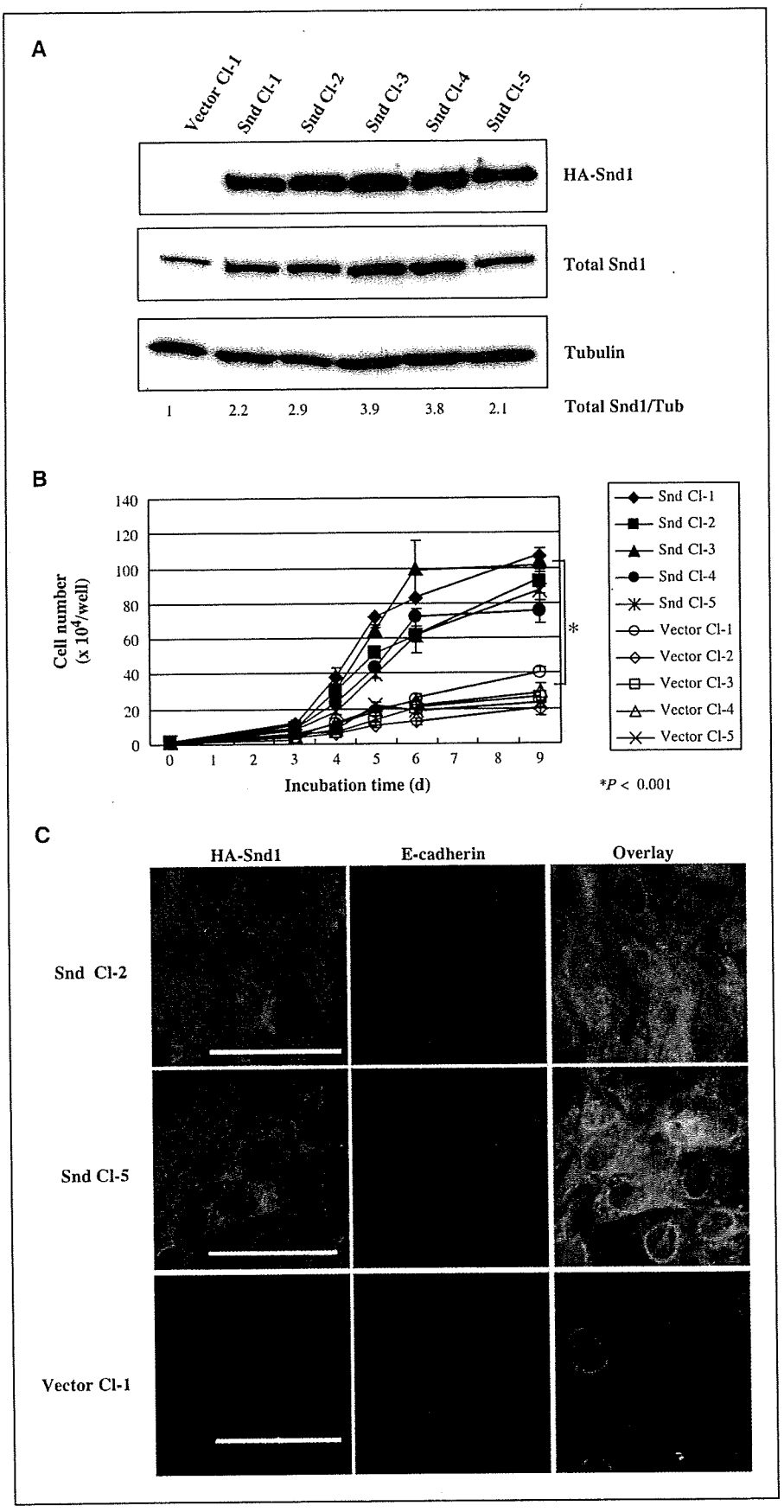

Figure 2. Establishment of the IEC-Snd cells. *A*, immunoblot analysis of recombinant HA-Snd1 expressed in IEC-Snd cells. Snd1-transfected IEC6 clones (a series of IEC-Snd clones; IEC-Snd Cl-1 to Cl-5) and a Vector-transfected clone (IEC-Vector Cl-1) were lysed in Laemmli's SDS sample buffer and subjected to immunoblot analysis. *Top*, HA-Snd1; *middle*, total Snd1 (endogenous Snd1 plus HA-Snd1); *bottom*, loading control tubulin. *Lane 1*, IEC-Vector Cl-1; *Lanes 2 to 6*, IEC-Snd Cl-1, Snd Cl-2, Snd Cl-3, Snd Cl-4 and Snd Cl-5, respectively. *B*, cell proliferation analysis. IEC-Snd and IEC-Vector cell clones were seeded on a 24-well plate at 2.5×10^4 cells/mL (0.5 mL/well), and the cell numbers were counted at indicated time points. The culture medium was changed at days 4 and 7. The data indicate the average with SD of a 4-well culture. Statistical analysis carried out by the Dunnett's test. *C*, localization of E-cadherin in IEC-Snd cells. IEC-Snd Cl-2 and Cl-5 and IEC-Vector Cl-1 cells, seeded on the glass-bottom dishes, were fixed with methanol and subjected to immunostaining, as detailed in Materials and Methods, and subjected to fluorescence microscopic analysis. Magnification, ×400; white bars, 50 μm.

Table 1. The colony number for each IEC-Snd clone on soft agar plate

Clones	No. colonies (per well)
Snd Cl-1	484
Snd Cl-2	513
Snd Cl-3	151
Snd Cl-4	76
Snd Cl-5	131
Vector Cl-1	10
Vector Cl-2	0
Vector Cl-3	2
Vector Cl-4	4
Vector Cl-5	13

NOTE: Detailed method is described in the legend to Supplementary Fig. S3.

due to the differences in cellular context between cell culture system and *in vivo* tissues. In other words, translocation of E-cadherin in transformed cancer cells in tissues might require additional genetic and/or epigenetic alterations after the accumulation of Snd1 and β-catenin.

It is well known that the *APC* gene is mutated or deleted in the majority of human colon cancers. Mutant forms of the APC protein cause activation of the Wnt-β-catenin signaling pathway and enhance the expression of cyclin D1 and c-myc oncogenes leading to development and progression of colorectal cancers (37). Activation of the Wnt-β-catenin signal pathway by *Apc* mutations has been observed in colon adenomas and occasionally in ACF (38, 39). In recent studies by Luchtenborg et al., however, *APC* mutations were detected in only 37% of human colon cancer cases, and the incidence of β-catenin mutations affecting phosphorylation sites was only 5 of 464 cases (1.1%; 40). Moreover, the mutation frequency in the *Apc* gene is much less frequent in colon cancers induced in rodents by chemical carcinogens, and ~30% to 40% of the cases do not harbor mutations in either *Apc* or *β-catenin* gene (41, 42). However, down-regulation of the *Apc* protein was frequently observed in azoxymethane- and PhIP-induced colon cancers (ref. 43 and our unpublished observation), despite the rare occurrence of *Apc* mutations (41, 42). Therefore, other unknown mechanisms have been considered to be involved, at least in part, in the activation of the Wnt-β-catenin signaling pathway. Down-regulation of the APC protein by SND1 overexpression could be an alternative molecular mechanism acting in the initial stages of colon carcinogenesis.

An important subject to be addressed is how Snd1 down-regulates the Apc protein. Although we currently do not have a clear idea on this point, gene-specific translational repression of tumor suppressor protein has been shown in several human cancer cells. For example, CAAT/enhancer binding protein α, a critical factor for myeloid cell differentiation, was suppressed in BCR/ABL-positive chronic myelogenous leukemia cells by the poly r(C)-binding heterogeneous ribonucleoprotein E2 (hnRNP E2; 44). hnRNP E1, a family member of hnRNP E2, is also known to bind to the differentiation control element of the 3′-untranslated region in the lipoxigenase mRNA (45). In colon cancer cells, thymidylate synthase is reported to bind to p53 mRNA and repress translation. Down-regulation of p53 protein levels in thymidylate synthase overexpressing human colon cancer cell lines has also been described (46). These previous findings and our current results point to an intriguing and novel scenario, whereby gene-specific suppression of translation could serve as part of critical initial events in the development of colon cancers. To prove, however, whether the translational repression by SND1 is exerted in either a

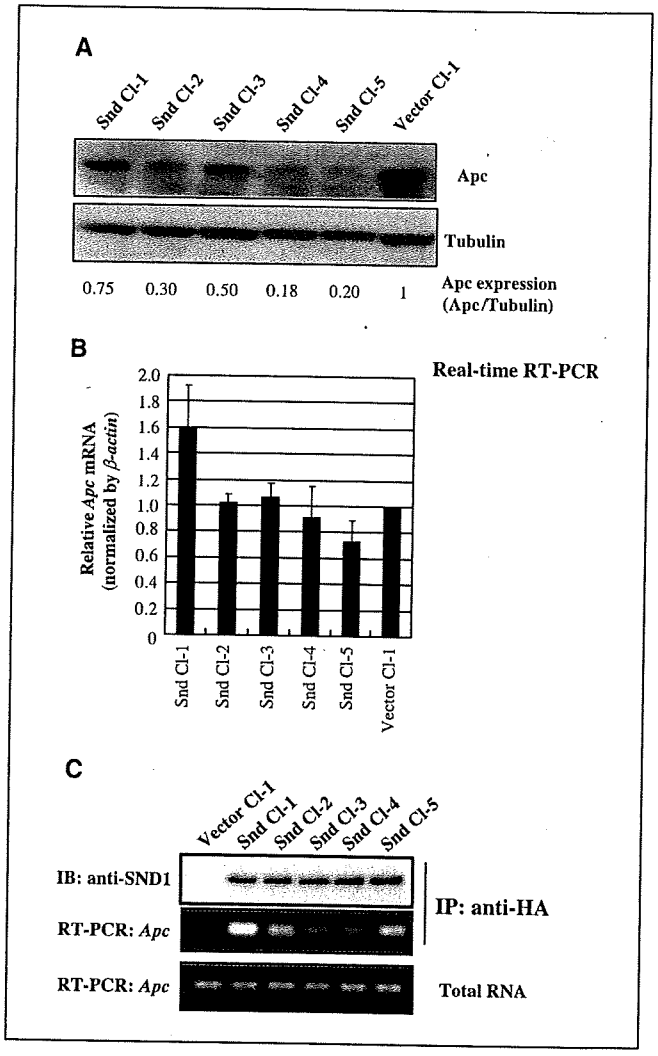

Figure 3. Down-regulation of the Apc protein without a significant change of *Apc* mRNA level in IEC-Snd clones. *A*, immunoblot analysis of the Apc protein in IEC-Snd clones. IEC-Snd and IEC-Vector clones were lysed in Laemmli's SDS sample buffer and subjected to immunoblot analysis. Immunoblot analysis of Apc (*top*) and control tubulin (*bottom*). The relative amounts of Apc were calculated by dividing the band densities of Apc by those of tubulin, which were determined by LAS3000 image analyzer and image gauge software (Fuji Film; *bottom*). *Lanes 1* to *5*, IEC-Snd Cl-1 to Cl-5, respectively; *lane 6*, IEC-Vector Cl-1. *B*, quantitative real-time PCR. Total RNAs from each IEC-Snd clones were subjected to reverse-transcriptase reaction using oligo(dT) primer and SuperScript II RT (Invitrogen). First strand of cDNA was subjected to PCR analysis using Apc and β-actin primer sets using Power SYBR Green PCR Mater Mix (Applied Biosystems). The relative amounts of *Apc* mRNA were normalized to those of β-actin. *C*, interaction of Snd1 with *Apc* mRNA. HA-Snd1 was precipitated using anti-HA agarose beads, and Snd1-bound RNAs were purified and subjected to RT-PCR analysis. *Top* and *middle*, immunoblot and RT-PCR analyses of immunoprecipitates from IEC-Snd clones, respectively; *bottom*, RT-PCR analysis of total RNA from each IEC clone.

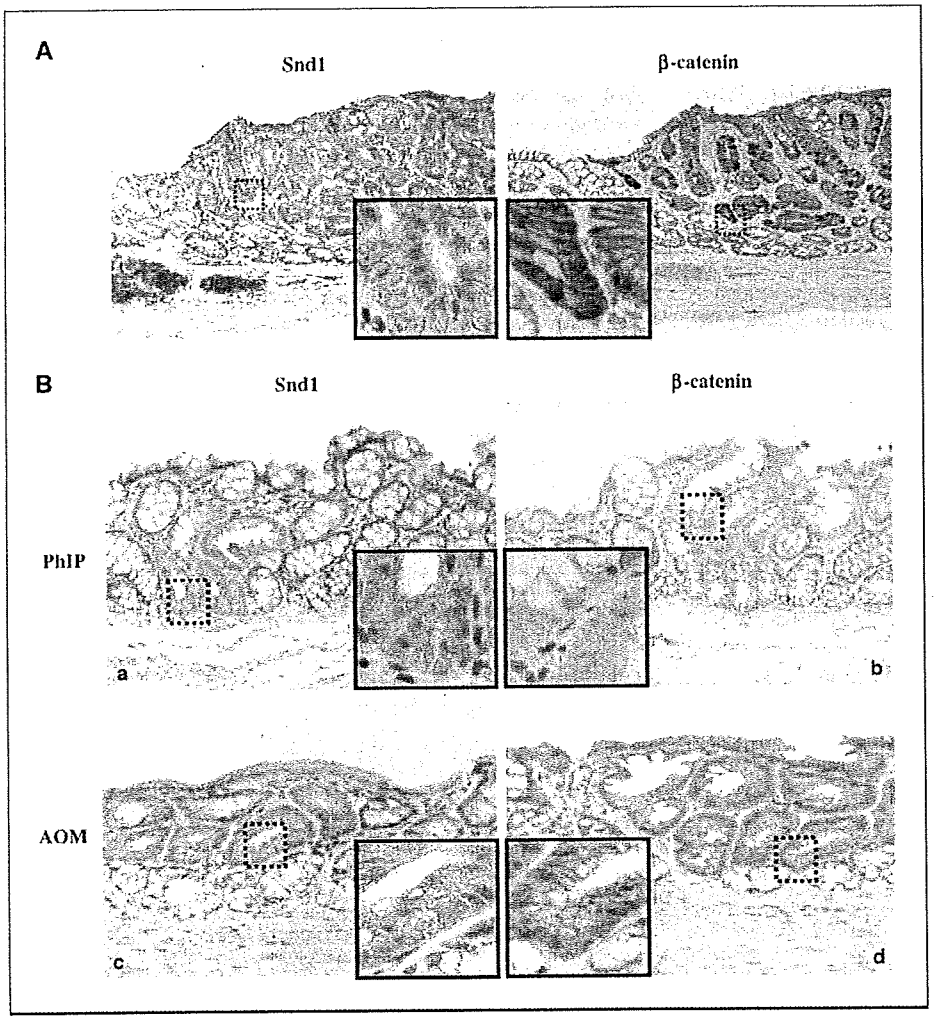

Figure 4. Accumulation of Snd1 and β-catenin in the cytoplasm of dysplastic ACF. *A*, serial paraffin sections of a colon tumor induced by azoxymethane were subjected to immunohistochemical analysis using anti-SND1 polyclonal antibody. The accumulation of Snd1 and β-catenin in the cancerous region. Enlarged images of the accumulation of Snd1 and β-catenin were included in the box of each image. Magnifications are ×100 and ×400. Enlarged region was marked by the square with dotted lines. *B*, serial paraffin sections of dysplastic ACF induced by PhIP (*a*, *b*) and those by azoxymethane (*c*, *d*) were subjected to immunohistochemical analysis using an anti-SND1 polyclonal antibody. *a and c*, marked accumulation of Snd1 is clear in the cytoplasm of two dysplastic ACF; *b*, *d*, cytoplasmic accumulation of β-catenin is faint in one (*b*), but moderate in the other lesion (*d*). Cytoplasmic accumulations of Snd1 and β-catenin were visualized by enlarged images in the box, and enlarged regions were marked by squares with dotted lines. Magnifications are ×100 and ×400.

gene-specific or nonspecific (or global) manner requires further study. Taking into consideration the present observation that SND1 overexpression did not induce a significant decrease in the β-catenin or tubulin protein levels, it is highly plausible that SND1 exerts its biological function as a translational repressor in some gene-specific manner.

We should also emphasize that SND1 may not be a sole regulator for the cellular APC protein level because the extent of

Table 2. Immunohistologic analysis for Snd1 and β-catenin in ACF induced by PhIP and azoxymethane

	Types of lesions	No. lesions analyzed	Status of β-catenin localization*		No. lesions with Snd1 accumulation
PhIP	Nondysplastic ACF	12	Cytoplasm	2†	2
			Membrane	10	5
	Dysplastic ACF	6	Cytoplasm	4	4
			Membrane	2	2
Azoxymethane	Nondysplastic ACF	5	Cytoplasm	0‡	
			Membrane	5	3
	Dysplastic ACF	18	Cytoplasm	12	12
			Membrane	6	5

*Lesions demonstrating β-catenin localization at the cytoplasm were considered to be positive for β-catein accumulation and those with membrane localization were estimated to be negative.

† Among 12 nondysplastic ACF induced by PhIP, two were selected because they showed the accumulation of β-catein in the cytoplasm. The remaining 10 lesions were randomly selected and subjected to immunohistochemical analysis.

‡ Among five nondysplastic ACF induced by azoxymethane, no accumulation of β-catenin in cytoplasm were detected.

down-regulation of Apc protein does not necessarily correlate with the Snd1 protein levels in IEC-Snd1 clones. SND1 may regulate *APC* mRNA translation in cooperation with other translational regulators. Furthermore, growth rates and the soft-agar colony formation activity of IEC-Snd clones did not completely correlate either with the total amount of Snd1 or with the Apc protein levels, indicating that SND1 could also be involved in translational regulation of other mRNAs associated with cell proliferation. Identification of other target mRNA species and interacting partners of SND1 protein should provide us with further insights into more precise roles of SND1 in colon carcinogenesis. Sequence-specific binding of Snd1 to single-stranded oligonucleotides (23) may contribute to this feature.

Another intriguing aspect of SND1 is its role as a possible component of RISC, and it indeed binds to some microRNA species (ref. 24 and our unpublished observation). Recently, gene specific translational control induced by microRNA species has been reported to have an effect on cancer development and progression (13). The expression profiles of microRNA in cancer tissues provided new insight into cancer diagnosis and prognosis and also into their roles in carcinogenesis (47–50). Although abnormality of microRNA gene expression is now an accepted signature of various cancers, functional analysis of effector RISC remains to be done. Aberrant regulation of microRNAs by RISC might also induce the malignant phenotype of cells. SND1 may thus control gene expression of APC or other cancer-related genes through control of microRNA–induced translational repression.

In summary, we report here, for the first time, that overexpression of SND1, a component of RISC, suppresses APC protein levels via posttranscriptional mechanisms. Functional activation of SND1 could be a novel mechanism underlying the initial development of precancerous lesions in the colon and contribute in an important way to the development of colon cancers at their very early stages.

Acknowledgments

Received 7/24/2006; revised 7/20/2007; accepted 7/25/2007.

Grant support: Ministry of Health, Labour and Welfare of Japan, Princess Takamatsu Cancer Research Fund, and Ministry of Education, Culture, Sports, Science and Technology of Japan (H. Nakagama).

The costs of publication of this article were defrayed in part by the payment of page charges. This article must therefore be hereby marked *advertisement* in accordance with 18 U.S.C. Section 1734 solely to indicate this fact.

We thank Dr. Roderick H. Dashwood (Oregon State University) for the critical review and comments on the manuscript.

References

1. Lengauer C, Kinzler KW, Vogelstein B. Genetic instabilities in human cancers. Nature 1998;396:643–9.
2. Baylin SB, Ohm JE. Epigenetic gene silencing in cancer - a mechanism for early oncogenic pathway addiction? Nat Rev Cancer 2006;6:107–16.
3. Oren M. Decision making by p53: life, death and cancer. Cell Death Differ 2003;10:431–42.
4. Alitalo K, Koskinen P, Makela TP, Saksela K, Sistonen L, Winqvist R. myc oncogenes: activation and amplification. Biochim Biophys Acta 1987;907:1–32.
5. Pandolfi PP. Aberrant mRNA translation in cancer pathogenesis: and old concept revisited comes finally of age. Oncogene 2004;23:3134–7.
6. Saito H, Hayday AC, Wilman K, Hayward WS, Tonegawa S. Activation of the c-myc gene by translation: a model for translational control. Proc Natl Acad Sci 1983;80:7476–80.
7. Landers JE, Haines DS, Strauss JF III, George DL. Enhanced translation: a novel mechanism of mdm2 oncogene overexpression identified in human tumor. Oncogene 1994;9:2745–50.
8. Takagi M, Absalon MJ, McLure KG, Kastan MB. Regulation of p53 translation and induction after DNA damage by ribosomal protein L26 and nucleolin. Cell 2005;123:49–63.
9. Smith MR, Jaramillo M, Liu YL, et al. Translation initiation factors induce DNA synthesis and transform NIH3T3 cells. New Biol 1990;2:648–54.
10. Ruggero D, Montanaro L, Ma L, et al. The translation factor eIF-4E promotes tumor formation and cooperated with c-Myc in lymphomagenesis. Nat Med 2004;10:484–6.
11. Corey DR. Regulating mammalian transcription with RNA. Trends Biochem Sci 2005;30:655–8.
12. Valencia-Sanchez MA, Liu J, Hannon GJ, Parker R. Control of translation and mRNA degradation by miRNAs and siRNAs. Genes Dev 2006;20:515–24.
13. Esquela-Kerscher A, Slack FJ. Oncomirs - microRNAs with a role in cancer. Nat Rev Cancer 2006;6:259–69.
14. Michael MZ, O'Connor SM, van Holst Pellekaan NG, Young GP, James RJ. Reduced accumulation of specific microRNAs in colorectal neoplasia. Mol Cancer Res 2003;1:882–91.
15. Calin GA, Sevignani C, Dumitru CD, et al. Human microRNA genes are frequently located at fragile sites and genomic region involved in cancers. Pro Natl Acad Sci 2004;101:2999–3004.
16. Calin GA, Ferracin M, Cimmino A, et al. A microRNA signature associated with prognosis and progression in chronic lymphocytic leukemia. N Engl J Med 2005;353:1793–17801.
17. Callebaut I, Mornon JP. The human EBNA-2 coactivator p100: multidomain organization and relation ship to the staphylococcal nuclease and to the tudor protein involved in Drosophila melanogaster development. Biochem J 1997;321:125–32.
18. Tong X, Drapkin R, Yalamanchili R, Mosialos G, Kieff E. The Epstein-Barr virus nuclear protein 2 acidic domain forms a complex with a novel cellular coactivator that can interact with TFIIE. Mol Cell Biol 1995;15:4735–44.
19. Dash AB, Orrico FC, Ness SA. The EVES motif mediates both intermolecular and intramolecular regulation of c-Myb. Genes Dev 1996;10:1858–69.
20. Yang J, Aittomaki S, Pesu M, et al. Identification of p100 as a coactivator for STAT6 that bridges STAT6 with RNA polymerase II. EMBO J 2002;21:4950–8.
21. Valineva T, Yang J, Palovuori R, Silvennoinen O. The transcriptional co-activator protein p100 recruits histone acetyltransferase activity to STAT6 and mediates interaction between CREB-binding protein and STAT6. J Biol Chem 2005;280:14989–96.
22. Fukuda H, Sugimura T, Nagao M, Nakagama H. Detection and isolation of minisatellite Pc-1 binding proteins. Biochim Biophys Acta 2001;1528:152–8.
23. Fukuda H, Tsuchiya N, Sato M, et al. DNA-binding activity of p100, a transcriptional co-activator, to single-stranded C-rich sequences. Proc Jpn Acad 2003;79B:120–3.
24. Caudy AA, Ketting RF, Hammond SM, et al. A micrococcal nuclease homologue in RNAi effector complexes. Nature 2003;425:411–4.
25. Notterman DA, Alon U, Sierk AJ, Levine AJ. Transcriptional gene expression profile of colorectal adenoma, adenocarcinoma, and normal tissue examined by oligonucleotide arrays. Cancer Res 2001;61:3124–30.
26. Ushigome M, Ubagai T, Fukuda H, et al. Up-regulation of hnRNP A1 gene in sporadic human colorectal cancers. Int J Oncol 2005;26:635–40.
27. Sambrook J, Fritsh EF, Maniatis T. Molecular cloning: A Laboratory manual. 2nd ed. Cold Spring Harbor (NY): Cold Spring Harbor Laboratory Press; 1989.
28. Laemmli UK. Cleavage of structural proteins during the assembly of the head of bacteriophage T4. Nature 1970;227:680–5.
29. Ubagai T, Ochiai M, Kawamori T, et al. Efficient induction of rat large intestinal tumors with a new spectrum of mutation by intermittent administration of 2-amino-1-methyl-6-phenylimidazo[4,5-*b*]pyridine in combination with a high fat diet. Carcinogenesis 2002;23:197–200.
30. Ochiai M, Ushigome M, Fujiwara K, et al. Characterization of aberrant crypt foci in the rat colon induced by 2-amino-1-methyl-6-phenylimidazo[4,5-*b*]pyridine, PhIP. Am J Pathol 2003;163:1607–14.
31. Ochiai M, Watanabe M, Nakanishi M, Taguchi A, Sugimura T, Nakagama H. Differential staining of dysplastic aberrant crypt foci in the colon facilitates prediction of carcinogenic potential of chemicals in rats. Cancer Lett 2005;220:67–74.
32. Segditsas S, Tomlinson I. Colorectal cancer and genetic alteration in the Wnt pathway. Oncogene 2006;25:7531–7.
33. Sharama C, Pradeep A, Wong L, Rana A, Rana B. Peroxisome proliferators-activated receptor γ activation can regulate β-catenin levels via a proteasomal-mediated and adenomatous polyposis coli-independent pathway. J Biol Chem 2004;279:35583–94.
34. Faux MC, Ross JL, Meeker C, et al. Restoration of full-length adenomatous polyposis coli (APC) protein in a colon cancer cell line enhances cell adhesion. J Cell Sci 2004;117:427–39.
35. Chang WW. Morphological basis of multistep process in experimental colonic carcinogenesis. Virchows Arch B [Cell Pathol] 1982;41:17–37.
36. Oshima H, Oshima M, Kobayashi M, Tsutsumi M, Taketo MM. Morphological and molecular processes of polyp formation in Apc (Δ716) knockout mice. Cancer Res 1997;57:1644–9.
37. Pint D, Clevers H. Wnt, stem cells and cancer in the intestine. Biol Cell 2005;97:185–96.
38. Takayama T, Ohi M, Hayashi T, et al. Analysis of K-ras, APC, β-catenin in aberrant crypt foci in sporadic adenoma, cancer, and familial adenomatous polyposis. Gastroenterology 2001;121:599–611.
39. Pretlow TP, Pretlow TG. Mutant KRAS in aberrant crypt foci (ACF): initiation of colorectal cancer? Biochim Biophys Acta 2005;1756:83–96.
40. Luchtenborg M, Weijenberg MP, Wark PA, et al. Mutation in APC, CTNNB1 and K-ras genes and expression of hMLH1 in sporadic colorectal carcinomas from the Netherlands Cohort Study. BMC Cancer 2005;5:160–70.

41. Takahashi M, Wakabayashi K. Gene mutations and altered gene expression in azoxymethane-induced colon carcinogenesis in rodents. Cancer Sci 2004;95: 475–80.
42. Nakagama H, Nakanishi M, Ochiai M. Modeling human colon cancer in rodents using a food-borne carcinogen, PhIP. Cancer Sci 2005;96:627–36.
43. Maltzman T, Whittington J, Driggers L, Stephens J, Ahnen D. AOM-induced mouse colon tumors do not express full-length APC protein. Carcinogenesis 1997;18: 2435–9.
44. Perrotti D, Cesi V, Trotta R, et al. BCR-ABL suppresses C/EBPα expression through inhibitory action of hnRNA E2. Nat Genet 2002;30:48–58.
45. Ostareck DH, Ostareck-Lederer A, Wilm M, Thiele BJ, Mann M, Hentze MW. mRNA silencing in erythroid differentiation: hnRNP K and hnRNP E1 regulates 15-lypoxygenase translation from the 3′ end. Cell 1997;89: 597–606.
46. Chu E, Copur SM, Ju J, et al. Thymidylate synthase protein and p53 mRNA form a *in vivo* ribonucleoprotein complex. Mol Cell Biol 1999;19:1582–94.
47. Lu J, Getz G, Miska FA, et al. MicroRNA expression profiles classify human cancers. Nature 2005;435:834–8.
48. Yanaihara N, Caplen N, Bowman E, et al. Unique microRNA molecular profiles in lung cancer diagnosis and prognosis. Cancer Cell 2006;9:189–98.
49. He L, Thomson JM, Hemann MT, et al. A microRNA polysistron as a potential human oncogene. Nature 2005;435:828–33.
50. Johnson SM, Grosshans H, Shingara J, et al. RAS is regulated by the let-7 microRNA family. Cell 2005;120: 635–47.

Mouse strain differences in inflammatory responses of colonic mucosa induced by dextran sulfate sodium cause differential susceptibility to PhIP-induced large bowel carcinogenesis

Masako Nakanishi,[1,3] Hiroshi Tazawa,[1] Naoto Tsuchiya,[1] Takashi Sugimura,[1] Takuji Tanaka[2] and Hitoshi Nakagama[1,4]

[1]Biochemistry Division, National Cancer Center Research Institute, 5-1-1 Tsukiji, Chuo-ku, Tokyo 104-0045; [2]Oncologic Pathology, Kanazawa Medical University, 1-1 Daigaku, Uchinada, Ishikawa 920-0293; [3]Department of Biochemistry, Osaka University Graduate School of Dentistry, 1-8 Yamadaoka, Suita, Osaka 565-0871, Japan

(Received December 22, 2006/Revised April 14, 2007/Accepted April 18, 2007/Online publication June 13, 2007)

In mice, 2-amino-1-methyl-6-phenylimidazo[4,5-*b*]pyridine (PhIP) induces a high incidence of malignant lymphoma and leukemia, but exhibits little, if any, carcinogenic activity in the large intestine after long-term exposure. However, recent studies have revealed that colonic adenocarcinomas can be efficiently and rapidly induced by combined treatment with PhIP and dextran sulfate sodium (DSS), a potent inducer of colitis. In the present study, the authors investigated the effects of inflammation on PhIP-induced carcinogenesis using two mouse strains, C57BL/6J and MSM/Ms, showing distinct temporal profiles of inflammatory responses to DSS. A long-term carcinogenesis experiment conducted with a single i.g. administration of PhIP (200 mg/kg body weight), followed by DSS treatment in drinking water for 4–6 days, revealed an increase in tumor incidence in C57BL/6J mice in accordance with the DSS intake. In contrast, neoplastic lesions were rarely observed in the MSM/Ms strain. From the short-term exposure to DSS for 4 days, C57BL/6J mice demonstrated severe chronic colitis, accompanied by hyperplastic cryptal epithelium and extensive cellular infiltration. Splenomegaly and swelling of mesenteric lymph nodes were also evident for over 1 month as chronic symptoms of systemic immunological disturbance. However, no inflammatory lesions were detected in MSM/Ms mice. The present results provide strong evidence that prolonged chronic inflammatory responses induced by DSS are directly responsible for the observed enhancement of PhIP-induced large bowel carcinogenicity. (*Cancer Sci* 2007; 98: 1157–1163)

HCA produced in cooked meat and fish show mutagenicity and carcinogenicity in experimental animals.[1–3] For example, PhIP, one of the most abundant HCA, induces colon, prostate, and mammary carcinomas in rats with long dietary exposure.[4] Because humans are exposed to various HCA in ordinary life, investigations of the molecular mechanisms underlying carcinogenesis by these genotoxic compounds and environmental modulators, such as bowel inflammation, high calorie intake and high-fat diet, are essential for evidence-based prevention efforts.

Animal models have major advantages for the analysis of molecular events during carcinogenesis and effects of both exogenous modifiers and genetic traits for cancer susceptibility. PhIP-induced rat colon cancers resemble human neoplasms with regard to multistage development and genetic alterations.[5,6] In mice, however, administration of PhIP mainly induces non-epithelial malignancies, such as malignant lymphomas and leukemia.[7–9] Although small intestinal tumors are occasionally induced in certain strains of mice given PhIP,[9] there have been no reports so far of large bowel carcinogenicity from treatment with PhIP alone.

Recently, Tanaka *et al.* developed a novel mouse model for inflammation-related colon carcinogenesis using a single, low-dose administration of chemicals, followed by treatment with a potent tumor-promoter, DSS, in drinking water.[10] DSS is a synthetic sulfated polysaccharide known to induce colitis on oral administration in mice,[11,12] rats,[13] hamsters,[14] and guinea pigs.[15,16] Because this model developed by Tanaka *et al.* is highly sensitive for inducing colon cancers,[10] chemicals with weak colonic carcinogenicity can also be detected within a short period of time. This has already proved to be the case for PhIP.[17] The DSS-induced colon cancer model indicates that bowel inflammation has a significant impact on the occurrence of colon cancers after exposure to environmental genotoxic compounds, and may serve as a powerful system for dissection of molecular mechanisms of, for example, IBD-related colon carcinogenesis in humans.

There have been many reports concerning links between inflammation and cancer.[18–20] In humans, the risk of colorectal neoplasia increases in good correlation with the extent and duration of inflammation in ulcerative colitis, one of the most common IBD.[19–22] In rodents, it has also been demonstrated that DSS-induced colitis promotes the development of colonic neoplasm in animals harboring hereditary genetic defects, such as *p53* deficiency or mutations in *Apc*.[23–25] Nevertheless, molecular mechanisms involved in the participation of inflammatory processes in carcinogenesis remain poorly defined. In the present study, the authors investigated the differences in the DSS-induced inflammatory responses in colonic mucosa in two mouse strains, C57BL/6J and MSM/Ms, and revealed their impact on PhIP-induced colon carcinogenesis.

Materials and Methods

Animals and chemicals. Two mouse strains were used: C57BL/6J and MSM/Ms. The C57BL/6J mice were obtained from CLEA Japan (Tokyo, Japan) and the MSM/Ms mice were obtained from the National Institute of Genetics (Mishima, Japan). The MSM/Ms mice are an inbred strain derived from Japanese wild mice (*M. molossinus*). C57BL/6J mice aged 7 weeks and MSM/Ms mice aged 7–9 weeks were maintained in an animal room with free access to drinking water and a powdered basal diet (AIN-93G; Dyets, Bethlehem, PA, USA), under controlled conditions and a 12:12-h light–dark cycle. This study was approved by the Institutional Animal Care and Use Committee at

[4]To whom correspondence should be addressed.
E-mail: hnakagam@gan2.res.ncc.go.jp

Abbreviations: ABC, avidin–biotin–peroxidase complex; AOM, azoxymethane; BW, body weight; DSS, dextran sulfate sodium; HCA, heterocyclic amines; IBD, inflammatory bowel disease; IFN, interferon; IL, interleukin; PBS, phosphate-buffered saline; PCNA, proliferating cell nuclear antigen; PhIP, 2-amino-1-methyl-6-phenylimidazo[4,5-*b*]pyridine; Rb, retinoblastoma.

doi: 10.1111/j.1349-7006.2007.00528.x

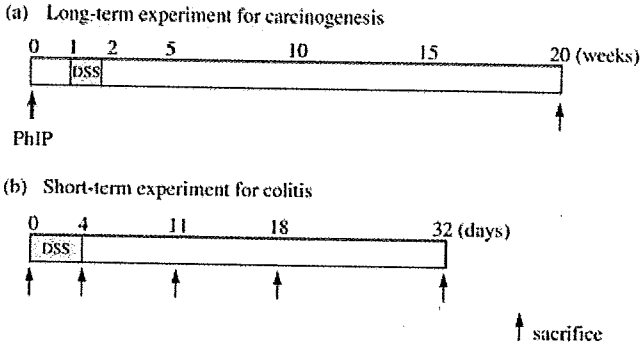

Fig. 1. Experimental protocols. (a) Long-term experiment for colon carcinogenesis. Mice were given a single i.g. administration of 2-amino-1-methyl-6-phenylimidazo[4,5-*b*]pyridine (PhIP) at a dose of 200 mg/kg body weight, followed by 1.0, 1.5, or 2.0% dextran sulfate sodium (DSS) in their drinking water for 4–6 days. Mice were killed when they become moribund, and the entire experiment was terminated at week 20. (b) Short-term experiment for DSS-induction of colitis. Mice at 7–9 weeks of age were administered 2.0% DSS (for the C57BL/6J mice) or 1.5% DSS (for the MSM/Ms mice) in their drinking water for 4 days, and killed at days 0, 4, 11, 18 and 32.

the National Cancer Center. DSS (molecular weight 36 000–50 000) was obtained from ICN Biochemicals (Aurora, OH, USA). PhIP was purchased from the Nard Institute (Osaka, Japan).

Induction of large bowel tumors. C57BL/6J (19 male and 16 female) and MSM/Ms mice (11 male and 17 female) were divided into two groups each and were given a single i.g. administration of PhIP (200 mg/kg BW). Some animals (3 of 35 C57BL/6J and 1 of 28 MSM/Ms mice) died immediately after PhIP-intubation. Starting 1 week after PhIP administration, the remaining animals were given 2.0, 1.5 or 1.0% DSS in drinking water for 4–6 days, and then maintained without any further treatment (Fig. 1a). A substantial number of the MSM/Ms mice died, particularly those given 1.5% DSS treatment following PhIP administration, which suffered from hematochezia and emaciation after DSS treatment. Because the colons of these animals were unable to be evaluated histopathologically, these animals were eliminated from the long-term carcinogenesis study. Finally, a total of 32 C57BL/6J (16 male and 16 female) and 20 MSM/Ms mice (7 male and 13 female) were subjected to the carcinogenesis experiment. As the control groups, a single i.g. administration of PhIP (200 mg/kg BW) without DSS or 2.0% DSS for 1 week without PhIP was administered to each of 3 C57BL/6J mice. During the course of the carcinogenesis experiment, animals were killed when they became moribund, and the entire experiments were terminated at week 20 by ether overdose and exsanguination. The cecum and entire colon were resected, flushed with saline, and cut open longitudinally along the main axis and then fixed in 10% buffered formalin. When large bowel tumors were detected macroscopically, tumor tissues were resected along with the surrounding normal epithelium, embedded in paraffin and subjected to histopathological evaluation.

Analysis of DSS-induced colitis. Two mice strains, C57BL/6J and MSM/Ms, were subjected to the experiment of DSS-induced colitis. Female C57BL/6J mice were exposed to 2.0% DSS for 4 days and killed 0, 1, 2, or 4 weeks after DSS cessation (days 4, 11, 18, and 32, respectively; Fig. 1b). For the MSM/Ms strains, female mice were exposed to 1.5% DSS for 4 days and killed for analysis as described above. Tissue samples from healthy control animals were acquired at day 0. The cecum and colon were removed and fixed as described above. The colon was divided into three segments (proximal, middle, and distal). Each segment of the colon and cecum was further dissected evenly into three longitudinal strips and embedded in paraffin for histological analysis.

Histopathological evaluation of colitis. The sections of each segment were stained with HE, and inflammation scores were determined from the intensity of inflammation as follows: grade 0, intact mucosa; grade 1, focal inflammatory infiltration; grade 2, inflammatory cell infiltration, gland dropout and crypt abscess formation; and grade 3, mucosal ulceration (Fig. 2). The intensity of inflammation was graded 0–3 as described above, and the extent of the involved area was estimated as 0–100%.[11,23] The inflammation scores were determined for each segment, and the total score was calculated as the sum of the inflammation scores in all segments, as described previously.[11]

Immunohistochemistry. Immunohistochemical examination of β-catenin and PCNA was performed using the ABC method (Elite ABC kit; Vectastain, Vector Laboratories Inc., Burlingame, CA, USA). For β-catenin immunostaining, deparaffinized sections were pretreated by autoclaving for 10 min in 10 mM citrate buffer (pH 6.0), and endogenous peroxidase activity was blocked by 3.0% H_2O_2 for 10 min. Sections were blocked with 5.0%

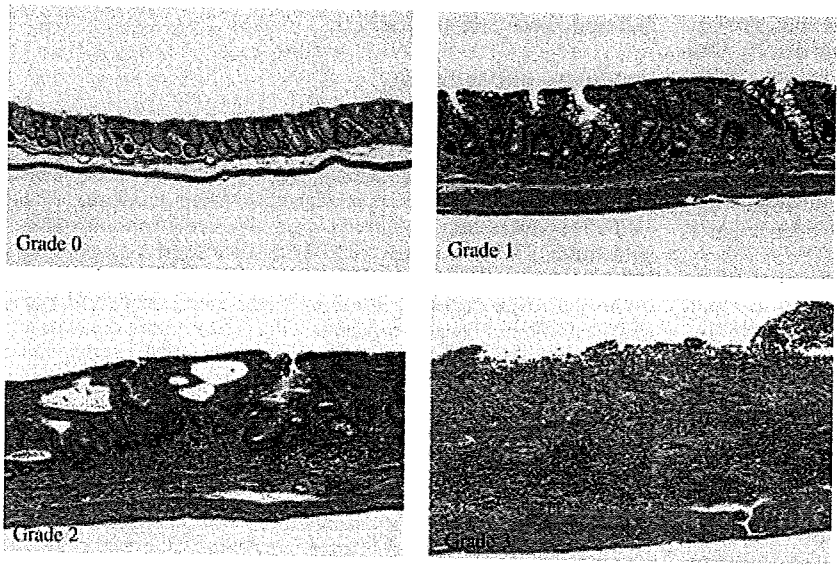

Fig. 2. Grading of inflammation (0, normal; 1, focal inflammatory infiltration; 2, moderate inflammation and gland dropout; 3, ulceration) and extent of involvement estimated as the percentage surface area (HE, ×100).

doi: 10.1111/j.1349-7006.2007.00528.x

Table 1. Induction of large bowel tumors in C57BL/6J and MSM/Ms mice

Mouse strain	Dose of DSS (duration)	DSS intake†	No. of mice surviving after PhIP treatment (at week 1)	No. of mice surviving after PhIP + DSS treatment (at week 3)	No. of mice with tumors (%)	Multiplicity of tumor/mouse
C57BL/6J	2.0% (6 days)	0.28 ± 0.01	14	14	7 (50)	1.00 ± 1.30*
MSM/Ms	1.5% (4 days)	0.32 ± 0.03	11	6	1 (17)	0.17 ± 0.17
C57BL/6J	1.5% (5 days)	0.20 ± 0.02	18	18	3 (17)	0.17 ± 0.38
MSM/Ms	1.0% (4 days)	0.19 ± 0.02	16	14	0 (0)	0

*$P < 0.05$ compared with 1.5% DSS-treated MSM/Ms mice. †The value of dextran sulfate sodium (DSS) intake was determined as mean ± standard error (g/day/100 g BW).

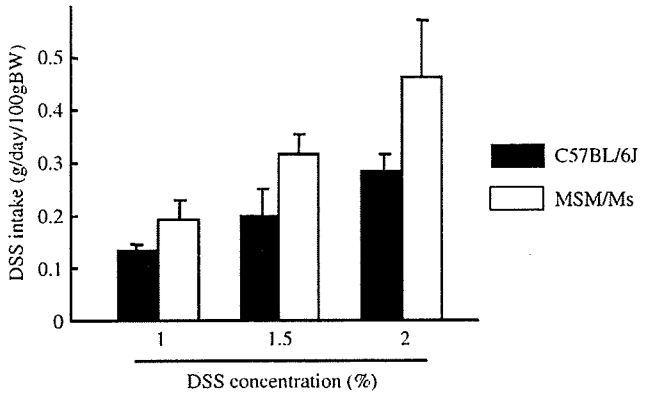

Fig. 3. Dextran sulfate sodium (DSS) intake levels corrected for body weight in C57BL/6J and MSM/Ms mice.

skimmed milk in PBS for 30 min, and then incubated for 1 h at room temperature with anti-β-catenin monoclonal antibody (diluted 1:200, BD Transduction Laboratories, Mississanga, ON, USA). For detection of PCNA labeling, deparaffinized sections were treated with microwave for 5 min in 10 mM citrate buffer, and incubated with 3.0% H_2O_2 for 10 min. Subsequently, sections were treated for 1 h in Mouse Ig Blocking Reagent (MOM™ Immunodetection Kit; Vector Laboratories) and then incubated for 1 h at room temperature with anti-PCNA monoclonal antibody (prediluted; Dako, Carpinteria, CA, USA). All sections were then treated with biotinylated secondary antibody for 30 min, followed by the reaction with Vectastain Elite ABC reagent for 30 min. After rinsing in PBS, 3,3-diaminobenzidine-tetrahydrochloride was used as a substrate for visualization of the immunocomplex, and the sections were counterstained with hematoxylin.

The percentage of cells reacting to PCNA was calculated in the order of 800 epithelial cells in each distal colon sample.

Statistical analysis. Data obtained were presented as means ± standard error. Paired samples were evaluated using Student's *t*-test. $P < 0.05$ was considered significant.

Results

Evaluation of DSS intake in C57BL/6J and MSM/Ms mice. DSS intake was evaluated during a 4-day period of 1.0%, 1.5% and 2.0% DSS administration for C57BL/6J and MSM/Ms mice, and the DSS intake per animal for all groups is shown in Fig. 3. Because the weight of the MSM/Ms mice was approximately half those of the C57BL/6J mice, the DSS intake was almost the same between the 1.0% MSM/Ms group and the 1.5% C57BL/6J group, and between the 1.5% MSM/Ms and 2.0% C57BL/6J groups. Based on DSS intake, the 2.0% DSS and 1.5% C57BL/6J mice were compared with the 1.5% and 1.0% DSS MSM/Ms groups, respectively, after administration of PhIP in the long-term experiment for colon carcinogenesis. Furthermore, the 2.0% DSS C57BL/6J group was compared with the 1.5% DSS MSM/Ms group in the short-term experiment for colitis.

General observations in the long-term carcinogenesis experiment. In the carcinogenesis experiment, groups of mice were given DSS at a concentration of 1.0, 1.5, or 2.0% 1 week after i.g. administration of PhIP (Fig. 1a). Some mice died immediately after the PhIP administration, as described in the Materials and Methods section. To the authors' surprise, MSM/Ms mice became highly sensitive to DSS when coadministered with PhIP, and showed lassitude and severe hematochezia during DSS treatment, leading to a high mortality rate. Of 11 and 16 MSM/Ms mice that survived after PhIP administration in the 1.5% DSS and 1.0% DSS groups, respectively, five and two animals died by week 3 (Table 1). In contrast, none of 32 C57BL/6J mice died either during or immediately after treatment with DSS. Their BW was transiently decreased by treatment with DSS.

Induction of large bowel tumors. The numbers of animals that could be analyzed for the long-term carcinogenesis experiment were finally determined to be 14 (2.0% DSS) and 18 (1.5% DSS) for the C57BL/6J strain, and 6 (1.5% DSS) and 14 (1.0% DSS) for the MSM/Ms strain, respectively. Data for the incidence and multiplicity of macroscopic colonic tumors in animals of each experimental group are summarized in Table 1. Before experimental termination at week 20, four C57BL/6J mice treated with 2.0% DSS developed large bowel tumors. The first large bowel tumor was noticed at week 5 because the mice manifested hematochezia and emaciation. A total of 17 colon tumors, either nodular or polypoid lesions, were induced in the C57BL/6J mice (14 in 2.0% DSS, and 3 in 1.5% DSS groups), and were diagnosed as adenomas or well-differentiated adenocarcinomas (Fig. 4a). The highest incidence was observed in the cecum (7/17, 41.2%), followed by the middle (6/17, 35.3%), distal (3/17, 17.6%), and proximal colon (1/17, 5.9%) (data not shown). In the MSM/Ms mice, an adenoma was found in only one MSM/Ms mouse treated with 1.5% DSS at week 20 (Table 1 and Fig. 4c). The multiplicity of tumor in 2.0% DSS-treated C57BL/6J mice was significantly ($P < 0.05$) increased compared with that in 1.5% DSS-treated MSM/Ms mice. C57BL/6J mice that received DSS alone without PhIP, or PhIP alone without DSS, had no tumors at these sacrifice points (data not shown).

Pathological findings for tumorigenesis. Besides the macroscopic colon tumors, the cecum and colon showed marked thickening of mucosa with mucosal ulceration at week 5 after PhIP administration in the C57BL/6J mice treated with 2.0% DSS. Adjacent to ulcers, hyperplastic epithelium without cellular atypism was occasionally observed (data not shown). However, the epithelial cells exhibited normal localization of β-catenin, suggestive of reactive hyperplasia rather than neoplasia (data not shown). Dysplastic focal lesions without mucosal hypertrophy were also observed in the C57BL/6J mice (Fig. 4b).

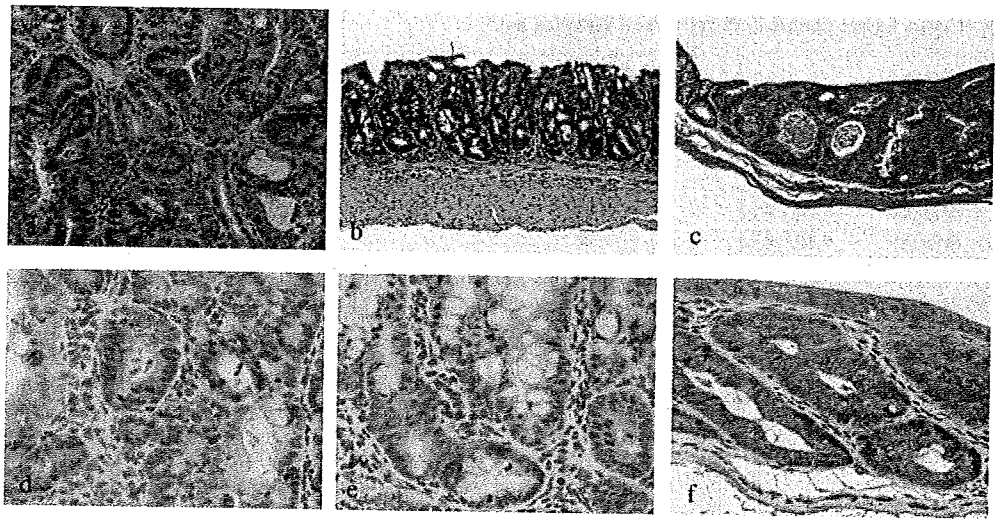

Fig. 4. Histopathology of colonic lesions in the C57BL/6J and MSM/Ms mice. (a,d) A tumor diagnosed as a well-differentiated adenocarcinoma in a C57BL/6J mouse. (b,e) A dysplastic focal lesion without mucosal hypertrophy was observed in a C57BL/6J mouse. (c,f) In the MSM/Ms mice, an adenoma was detected in a mouse at week 20. (d–f) Note translocation of β-catenin from the cell membrane to the cytoplasm and nucleus. (a–c) HE, ×100. (d–f) Immunohistochemistry, ×200.

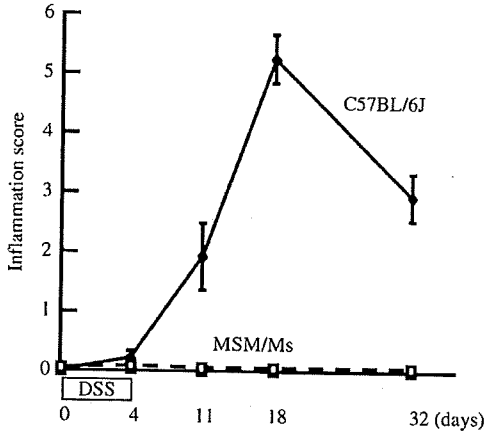

Fig. 5. Time-course of changes in inflammation scores. Histological evaluation of inflammation in the C57BL/6J and MSM/Ms mice treated with 2.0% and 1.5% dextran sulfate sodium (DSS), respectively, was performed using three mice at each time point. No significant colitis occurred in the MSM/Ms mice, whereas the C57BL/6J mice developed severe chronic inflammation.

Immunohistochemically, translocation of β-catenin from the cell membrane to the cytoplasm and nucleus was observed in tumor cells (Fig. 4d). Furthermore, accumulation of β-catenin was detected in the cytoplasm and the nucleus of dysplastic focal lesions (Fig. 4e). In the MSM/Ms mice, an adenoma was also accumulated with β-catenin (Fig. 4f).

Acute- and chronic-phase inflammatory responses to DSS. The C57BL/6J mice given 2.0% DSS transiently showed diarrhea and bloody stools from day 2, but these disappeared after cessation of DSS. As for the MSM/Ms mice, no clinical symptoms were evident from external observations in mice treated with either 1.5% or 1.0% DSS. The chronological change in inflammation scores in the C57BL/6J and MSM/Ms mice treated with 2.0% and 1.5% DSS, respectively, is illustrated in Fig. 5. In the acute-phase after DSS exposure (at day 4), early inflammatory responses, such as shortening of crypts and thinning/loss of cryptal cells without infiltration of inflammatory cells, were detected in C57BL/6J mice. MSM/Ms mice showed no significant colitis. In C57BL/6J mice, histological changes became much more severe at day 11, with shortening of the length of the colon accompanied by prominent hypertrophy of the mucosa.

In the chronic-phase of inflammation, differences were also observed between the C57BL/6J and MSM/Ms mice (Fig. 5). In the C57BL/6J case, the peak inflammation score was found at day 18, and multiple erosive lesions with infiltration of neutrophils and lymphocytes were observed in the cecum and colon. Mucosal hypertrophy resulting from reactive/regenerative hyperplasia of the epithelium was also observed. Although the severity of inflammation was slightly reduced at day 32, progression into chronic inflammation was demonstrated by infiltration of macrophages, lymphocytes, and plasma cells extensively distributed in the lamina propria and submucosa (Figs 5,6a). In contrast, MSM/Ms mice showed no significant colitis even in the chronic phase of inflammation (Figs 5,6b). By immunohistochemistry using anti-PCNA antibody, numerous cells showing positive nuclear reactions were present in hyperplastic epithelium in the C57BL/6J mice (Fig. 6e). The number of PCNA-positive cells was significantly increased ($P < 0.005$) at day 18 compared with that at day 0 in C57BL/6J mice, although MSM/Ms mice showed no change between the number of PCNA-positive cells at day 0 and at day 18 (Fig. 6g).

Inflammatory lesions in the C57BL/6J mice, including hyperplastic epithelium showing notable proliferative activity, were most prominent in the cecum, followed by the distal and middle colon (Fig. 7). In contrast, pathologic alterations were rarely found in the proximal colon. This is in good agreement with the topological differences in the tumor frequency of the large bowel. In addition to colitis, pathological changes occurred in C57BL/6J mice as a result of DSS treatment. Strikingly, enlarged spleens and mesenteric lymph nodes were found only in the C57BL/6J mice at day 11, and were maintained throughout to day 32 (data not shown). Enlargement of mesenteric lymph nodes was accompanied by aggregation of foamy macrophages and plasmacytosis. In the spleen and liver, extramedullary hematopoiesis was notably increased. In the other major organs, including kidneys, lungs, heart, pancreas, adrenal glands, and brain, there were no significant lesions. In contrast, the MSM/Ms mice exhibited neither the inflammatory responses nor the systemic changes observed in the C57BL/6J mice.

doi: 10.1111/j.1349-7006.2007.00528.x

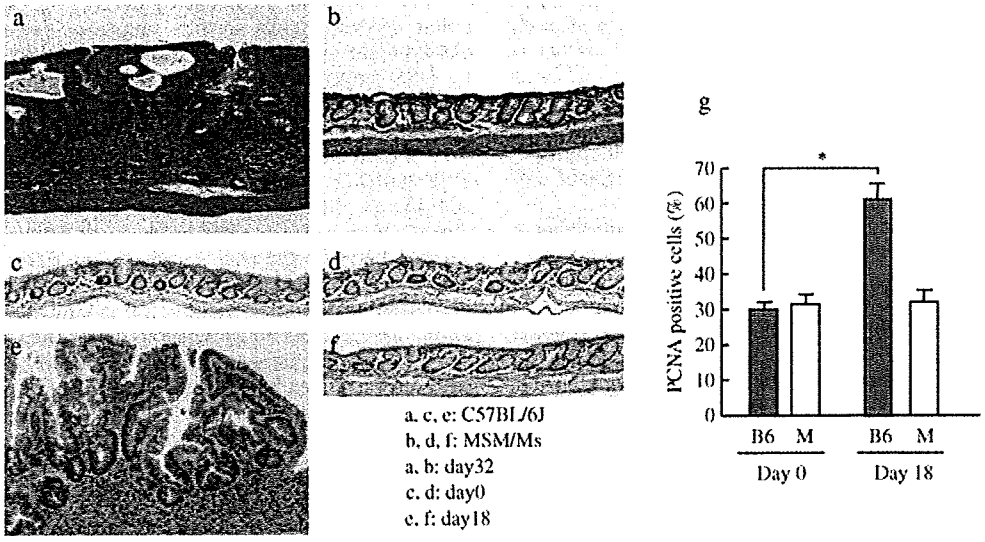

Fig. 6. Histopathology of the distal colon in C57BL/6J and MSM/Ms mice at late stage. Mucosal hypertrophy accompanied by regenerative epithelium and prominent infiltration of inflammatory cells is evident in (a) a C57BL/6J mouse, but not in (b) a MSM/Ms mouse at day 32. Proliferative activity of the epithelium was detected using immunohistochemistry with proliferating cell nuclear antigen (PCNA) antibodies in (c,e) C57BL/6J and (d,f) MSM/Ms mice at (c,d) day 0 and (e,f) day 18. (a,b) HE, ×100. (c–f) Immunohistochemisty, ×100. (g) The number of PCNA positive cells in C57BL/6J mice (B6) was significantly ($P < 0.005$) increased at day 18 compared with that at day 0. MSM/Ms mice (M) showed no change between the number of PCNA-positive cells at day 0 and at day 18.

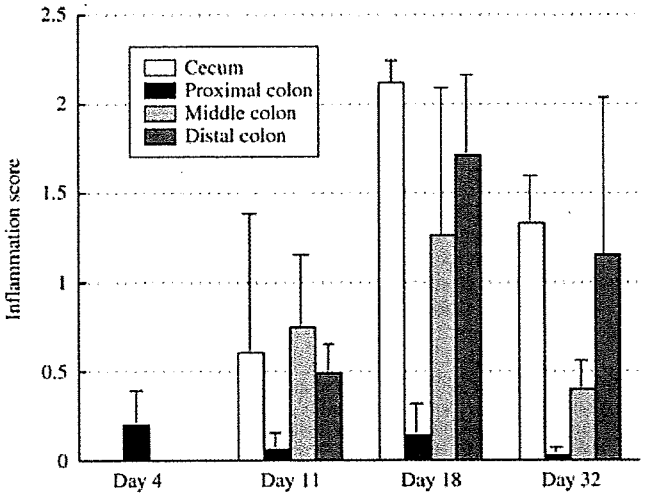

Fig. 7. Topological differences in the susceptibility to dextran sulfate sodium-induced colitis in the cecum and the colon. Inflammation scores were evaluated for the C57BL/6J mice at experimental days 4, 11, 18 and 32 as detailed in Materials and Methods. Inflammatory lesions were most prominent in the cecum, particularly at days 18 and 32 in the chronic phase, followed by the distal and middle colon. The inflammatory scores represented in this figure were cited and modified from our current report in the *Proceedings of the Japanese Society of Animal Models for Human Diseases* (Japanese) [Nakanishi M *et al.* July, 2006].

Discussion

Epidemiological studies to date have shown that human colon cancers are caused by both heritable genetic factors and various environmental influences,[26] and bowel inflammation has been considered to have a significant impact on the risk of human carcinogenesis.[19–22] While DSS is a non-genotoxic chemical, long-term treatment has been reported to induce colon tumors in rats, albeit at a low incidence.[27,28] DSS treatment acts as a powerful tumor promoter in mice and rats when combined with a genotoxic carcinogen.[10,28]

In the present study, it was clearly demonstrated that C57BL/6J mice showed higher susceptibility to colon carcinogenesis induced by combined administration of PhIP with DSS compared with MSM/Ms mice (Table 1), when DSS intake is similar in both strains. Furthermore, tumor incidence was increased in accordance with the DSS intake in both strains of mice. These results strongly suggest that DSS-induced inflammatory conditions may be involved in the strain difference of tumor development. In the short-term experiment, inflammation scores demonstrated substantial differences in the development of colitis between the two strains of mice. Changes in the acute phase, including crypt shortening and inflammatory cell infiltration, and in the chronic phase, including mucosal hypertrophy with progressive infiltration of inflammatory cells, were limited to the C57BL/6J strain, and this appeared to be linked to carcinogenesis. C57BL/6J mice also showed splenomegaly and swelling of mesenteric lymph nodes at days 18 and 32, suggesting that the systemic immune system was chronically disturbed in the C57BL/6J strain. This strain difference in the inflammatory status induced by DSS may contribute to differential susceptibility to PhIP-induced colon carcinogenesis in mice.

An interesting and original finding in the present study is that tumors with the greatest incidence developed in the cecum of the C57BL/6J mice that received DSS, where the inflammatory response was the most severe. Cooper *et al.* have also reported similar findings of severe inflammation in the cecum of female C57BL/6J and male C57BL6/J-Min mice that were given a single or cycle treatment of DSS, but unfortunately they did not describe the neoplastic lesions in the region.[23] Although the mechanism of the high frequency of tumor development in the cecum remains unclear, the high susceptibility of cecal lesions to inflammatory response may be involved in inflammation-associated tumor development. The cecal lumen contains many bacteria that are metabolically active in bioactivating or detoxifying compounds. Also, diffuse lymphatic tissue is abundant in the lamina propria of the cecum and is often observed in the submucosa. In addition,

cecal cryptal cell turnover is under immunological control by certain cytokines and chemokines.[29] The authors have recently observed the development of tumors in the inflamed cecum as well as in the colon of *Apc*$^{Min/+}$ mice treated with DSS (unpublished observations, 2006). Further studies are needed to determine the significance of these findings showing the significance of cecal inflammation on colon carcinogenesis, as cecal inflammatory conditions have been also shown to be strongly associated with the progression of distal ulcerative colitis of IBD.[30]

Animals orally administered DSS develop colitis with features similar to symptomatic and histological findings in human IBD.[31] Differential susceptibility to DSS-induced colitis in mice has been considered to be based mainly on strain differences in genetic background.[32] Similar to human IBD, many genes associated with inflammatory responses could be candidates for genetic susceptibility. Melgar *et al.* recently demonstrated that progressive up-regulation of plasma haptoglobin and cytokines, such as IL-1-α/-β, IL-6, IL-12, IL-17 and IFN-γ, occurs in the colon tissue of mice with DSS-induced colitis.[33] They found that C57BL/6 mice develop severe inflammation accompanied by continuous production of cytokines, but acute colitis was completely resolved in the BALB/c strain. Although the pathogenesis of DSS-induced colitis remains to be elucidated, local immunological disturbance,[34–36] activation of macrophages in the lamina propria,[12,16] obstruction or obliteration of the crypt lumina by accumulated mucus,[15] and/or changes in the intestinal microflora population,[12,13] could be causative.

C57BL/6J mice showed an increase in colon epithelial cells proliferating in the inflammatory tissues at day 18 after DSS treatment, whereas MSM/Ms mice exhibited no increase in them. These results suggest that stimulated cell proliferation by DSS may be also involved in colon carcinogenesis induced by PhIP and DSS. A recent study has shown the hyperphosphorylation of Rb protein associated with cell proliferation in the DSS-induced mouse colitis and human ulcerative colitis.[37] Rb phosphorylation was strongly associated with activation of E2F1-downstream target genes, including *PCNA*, *cyclin D1* and *Akt*. In the present study, activation of the Rb pathway may be involved in the cell proliferation induced by DSS, and accelerate the tumor development induced by PhIP and DSS as a result of proliferation of mutated cells. In contrast, administration of the antioxidant *N*-acetylcysteine suppressed colonic tumor development induced by long-term DSS treatment by decreasing the proliferation of colon epithelial cells in non-cancerous tissues.[38] Therefore, clarifying the molecular mechanism of stimulated cell proliferation by DSS may provide novel insights into the underlying processes and prevention of tumor development in inflammation-associated human colon carcinogenesis.

It should also be noted that combined administration of PhIP and DSS induced high mortality in the MSM/Ms strain. In addition to differential susceptibility to DSS-induced colitis, other factors, such as differences in PhIP-induced colonic cell damage between the two mouse strains might be involved. In rats, strain differences in susceptibility to PhIP carcinogenicity have been reported.[6,39] Similarly, it is known that different mice strains have distinct sensitivities to colon carcinogenesis induced by AOM, an alkylating agent.[40–42] Recently, strain differences were also indicated by Tanaka's group in AOM and DSS-induced colon carcinogenesis in mice.[43] Susceptibility to the induction of colon cancers by a combined treatment with AOM and DSS was not fully consistent with that for AOM single exposure, and Suzuki *et al.* stressed the direct contribution of nitrosation stress due to DSS-induced inflammation.[43]

In conclusion, the authors have shown a strain difference in the combined treatment with PhIP and DSS-induced colon carcinogenesis model in mice. C57BL/6J mice showing chronic progression of DSS colitis thus appear to be useful for analysis of IBD-associated neoplasia. Furthermore, investigation of strain differences in rodents might provide pointers to individual variation in humans. As part of ongoing studies in the authors' laboratory, genetic analysis of several consomic mouse strains is being carried out to identify susceptibility or resistance of genes to PhIP and DSS-induced carcinogenesis.

Acknowledgments

This work was supported in part by Grants-in-Aid for Cancer Research and for the Third Term Comprehensive Control Research for Cancer from the Ministry of Health, Labour and Welfare of Japan, and by a Grant-in-Aid for Scientific Research on Priority Area (C) from the Ministry of Education, Culture, Sports, Science and Technology of Japan. MN was the recipient of a Research Resident Fellowship from the Foundation for Promotion of Cancer Research in Japan during the performance of the work.

References

1 Nagao M, Ushijima T, Toyota M, Inoue R, Sugimura T. Genetic changes induced by heterocyclic amines. *Mutat Res* 1997; **376**: 161–7.
2 Sugimura T, Nagao M, Wakabayashi K. How we should deal with unavoidable exposure of man to environmental mutagens: cooked food mutagen discovery, facts and lessons for cancer prevention. *Mutat Res* 2000; **447**: 15–25.
3 Sugimura T, Wakabayashi K, Nakagama H, Nagao M. Heterocyclic amines. Mutagens/carcinogens produced during cooking of meat and fish. *Cancer Sci* 2004; **95**: 290–9.
4 Ohgaki H. 7.1 Rodents. In: Nagao M, Sugimura T, eds. *Food Borne Carcinogenesis: Heterocyclic Amines*. New York: John Wiley, 2000: 198–204.
5 Ubagai T, Ochiai M, Kawamori T *et al.* Efficient induction of rat large intestinal tumors with a new spectrum of mutations by intermittent administration of 2-amini-1-methyl-6-phenylimidazo[4,5-*b*]pyridine in combination with a high fat diet. *Carcinogenesis* 2002; **23**: 197–200.
6 Nakagama H, Ochiai M, Ubagai T *et al.* A rat colon cancer model induced by 2-amino-1-methyl-6-phenylimidazo[4,5-*b*]pyridine, PhIP. *Mutat Res* 2002; **506/507**: 137–44.
7 Esumi H, Ohgaki H, Kohzen E, Takayama S, Sugimura T. Induction of lymphoma in CDF1 mice by the food mutagen, 2-amino-1-methyl-6-phenylimizado[4,5-*b*]pyridine. *Jpn J Cancer Res* 1989; **80**: 1176–8.
8 Kristiansen E, Mortensen A, Sørennsen IK. Effect of long-term feeding with 2-amino-1-methyl-6-phenylimidazo[4,5-*b*]pyridine (PhIP) in C57BL/ByA and Eμ-*pin*-1 mice. *Cancer Lett* 1998; **122**: 215–20.
9 Ochiai M, Imai H, Sugimura T, Nagao M, Nakagama H. Induction of intestinal tumors and lymphomas in C57BL/6N mice by a food-borne carcinogen, 2-amino-1-methyl-6-phenylimidazo[4,5-*b*]pyridine. *Jpn J Cancer Res* 2002; **93**: 478–83.
10 Tanaka T, Kohno H, Suzuki R, Yamada Y, Sugie S, More H. A novel inflammation-related mouse colon carcinogenesis model induced by azoxymethane and dextran sodium sulfate. *Cancer Sci* 2003; **94**: 965–73.
11 Cooper HS, Murthy SNS, Shah RS, Sedergran DJ. Clinicopathologic study of dextran sulfate sodium experimental murine colitis. *Laboratory Invest* 1993; **69**: 238–49.
12 Okayasu I, Hatakeyama S, Yamada M, Ohkusa T, Inagaki Y, Nakaya R. A novel method in the induction of reliable experimental acute and chronic ulcerative colitis in mice. *Gastroenterology* 1990; **98**: 694–702.
13 Tamaru T, Kobayashi H, Kishimoto S, Kajiyama G, Shimamoto F, Brown WR. Histochemical study of colonic cancer in experimental colitis of rats. *Dig Dis Sci* 1993; **38**: 529–37.
14 Yamada M, Ohkusa T, Okayasu I. Occurrence of dysplasia and adenocarcinoma after experimental chronic ulcerative colitis in hamsters induced by dextran sulphate sodium. *Gut* 1992; **33**: 1521–7.
15 Iwanaga T, Hoshi O, Han H, Fujita T. Morphological analysis of acute ulcerative colitis experimentally induced by dextran sulfate sodium in the guinea pig: Some possible mechanisms of cecal ulceration. *J Gastroenterol* 1994; **29**: 430–8.
16 Hoshi O, Iwanaga T, Fujino MA. Selective uptake of intraluminal dextran sulfate sodium and senna by macrophages in the cecal mucosa of the guinea pig. *J Gastroenterol* 1996; **31**: 189–98.
17 Tanaka T, Suzuki R, Kohno H, Sugie S, Takahashi M, Wakabayashi K. Colon adenocarcinomas rapidly induced by the combined treatment with

doi: 10.1111/j.1349-7006.2007.00528.x

2-amino-1-methyl-6-phenylimidazo[4,5-*b*]pyridine and dextran sodium sulfate in male ICR mice possess *β-catenin* gene mutations and increased immunoreactivity for β-catenin, cyclooxygenase-2 and inducible nitric oxide synthase. *Carcinogenesis* 2005; **26**: 229–38.
18 Balkwill F, Mantovani A. Inflammation and cancer: back to Virchow? *Lancet* 2001; **357**: 539–45.
19 Itzkowitz SH, Yio X. Inflammation and cancer IV. Colorectal cancer in inflammatory bowel disease: the role of inflammation. *Am J Physiol Gastrointest Liver Physiol* 2004; **287**: G7–17.
20 Rutter M, Saunders B, Wilkinson K *et al*. Severity of inflammation is a risk factor for colorectal neoplasia in ulcerative colitis. *Gastroenterology* 2004; **126**: 451–9.
21 Munkholm P. Review article: the incidence and prevalence of colorectal cancer in inflammatory bowel disease. *Aliment Pharmacol Ther* 2003; **18**: 1–5.
22 Seril DN, Liao J, Yang G, Yang CS. Oxidative stress and ulcerative colitis-associated carcinogenesis: studies in humans and animal models. *Carcinogenesis* 2003; **24**: 353–62.
23 Cooper HS, Everley L, Chang W *et al*. The role of mutant *Apc* in the development of dysplasia and cancer in the mouse model of dextran sulfate sodium-induced colitis. *Gastroenterology* 2001; **121**: 1407–16.
24 Fujii S, Fujimori T, Kawamata H *et al*. Development of colonic neoplasia in *p53* deficient mice with experimental colitis induced by dextran sulfate sodium. *Gut* 2004; **53**: 710–16.
25 Tanaka T, Kohno H, Suzuki R *et al*. Dextran sodium sulfate strongly promotes colorectal carcinogenesis in $Apc^{Min/+}$ mice: Inflammatory stimuli by dextran sodium sulfate results in development of multiple colonic neoplasms. *Int J Cancer* 2006; **118**: 25–34.
26 Kolonel LN, Altshuler O, Henderson BE. The multiethnic cohort study: exploring genes, lifestyle and cancer resk. *Nat Rev Cancer* 2004; **7**: 519–27.
27 Whiteley LO, Hudson L, Pretlow TP. Aberrant crypt foci in the colonic mucosa of rats treated with genotoxic and nongenotoxic colon carcinogens. *Toxicol Pathol* 1996; **24**: 681–9.
28 Onose J, Imai T, Hasumura M, Ueda M, Hirose M. Rapid induction of colorectal tumors in rats initiated with 1,2-dimethylhydrazine followed by dextran sodium sulfate treatment. *Cancer Lett* 2003; **198**: 145–52.
29 Cliffe LJ, Humphreys NE, Lane TE, Potten CS, Booth C, Grencis RK. Accelerated intestinal epithelial cell turnover: a new mechanism of parasite expulsion. *Science* 2005; **308**: 1463–5.
30 D'Haens G, Geboes K, Peeters M, Baert F, Ectors N, Rutgeerts P. Patchy cecal inflammation associated with distal ulcerative colitis: a prospective endoscopic study. *Am J Gastroenterol* 1997; **92**: 1275–9.
31 Cooper HS, Murthy S, Kido K, Yoshitake H, Flanigan A. Dysplasia and cancer in the dextran sulfate sodium mouse colitis model. Relevance to colitis-associated neoplasia in the human: a study of histopathology, β-catenin and p53 expression and the role of inflammation. *Carcinogenesis* 2000; **21**: 757–68.
32 Mahler M, Bristol IJ, Sundberg JP *et al*. Genetic analysis of susceptibility to dextran sulfate sodium-induced colitis in mice. *Genomics* 1999; **55**: 147–56.
33 Melgar S, Karlsson A, Michaëlsson E. Acute colitis induced by dextran sulfate sodium progresses to chronicity in C57BL/6 but not in BALB/c mice: correlation between symptoms and inflammation. *Am J Physiol Gastrointest Liver Physiol* 2005; **288**: G1328–38.
34 Kobayashi K, Asakura H, Hamada Y *et al*. T lymphocyte subpopulations and immunoglobulin-containing cells in the colonic mucosa of ulcerative colitis; a morphometric and immunohistochemical study. *J Clin Laboratory Immunol* 1988; **25**: 63–8.
35 Powrie F, Leach MW. Genetic and spontaneous models of inflammatory bowel disease in rodents: evidence for abnormalities in mucosal immune regulation. *Ther Immunol* 1995; **2**: 115–23.
36 Tokoi S, Ohkusa T, Okayasu I, Nakamura K. Population changes in immunoglobulin-containing mononuclear cells in dextran sulfate sodium-induced colitis. *J Gastroenterol* 1996; **31**: 182–8.
37 Ying L, Marino J, Hussain SP *et al*. Chronic inflammation promotes retinoblastoma protein hyperphosphorylation and E2F1 activation. *Cancer Res* 2005; **65**: 9132–6.
38 Seril DN, Liao J, Ho KL, Yang CS, Yang GY. Inhibition of chronic ulcerative colitis-associated colorectal adenocarcinoma development in a murine model by *N*-acetylcysteine. *Carcinogenesis* 2002; **23**: 993–1001.
39 Ishiguro Y, Ochiai M, Sugimura T, Nagao M, Nakagama H. Strain differences of rats in the susceptibility to aberrant crypt foci formation by 2-amino-1-methyl-6-phenylimidazo[4,5-*b*]pyridine: no implication of *Apc* and *Pla2g2a* genetic polymorphisms in different susceptibility. *Carcinogenesis* 1999; **20**: 1063–8.
40 Wang QS, Walsh A, Goldsby JS, Papanikolaou A, Bolt AB, Rosenberg DW. Preliminary analysis of azoxymethane-induced colon tumorigenesis in mouse aggregation chimeras. *Carcinogenesis* 1999; **20**: 691–7.
41 Nambiar PR, Girnun G, Lillo NA, Guda K, Whiteley HE, Rosenberg DW. Preliminary analysis of azoxymethane induced colon tumors in inbred mice commonly used as transgenic/knockout progenitors. *Int J Oncol* 2003; **22**: 145–50.
42 Pereira MA, Tao LH, Wang W, Gunning WT, Lubet R. Chemoprevention: mouse colon and lung tumor bioassays and modulation of DNA methylation as a biomarker. *Exp Lung Res* 2005; **31**: 145–63.
43 Suzuki R, Kohno H, Sugie S, Nakagama H, Tanaka T. Strain differences in the susceptibility to azoxymethane and dextran sodium sulfate-induced colon carcinogenesis in mice. *Carcinogenesis* 2006; **27**: 162–9.